University of São Paulo
"Luiz de Queiroz" College of Agriculture

Use of bone char and biochar for recycling phosphorus into agricultural systems

Cristiano Dela Piccolla

Thesis presented to obtain the degree of Doctor in Science.
Area: Soils and Plant Nutrition

Piracicaba
2018

Cristiano Dela Piccolla
Agronomist

Use of bone char and biochar for recycling phosphorus into agricultural systems

versão revisada de acordo com a resolução CoPGr 6018 de 2011

Advisor
Prof. Dr. **TAKASHI MURAOKA**

Thesis presented to obtain the degree of Doctor in Science.
Area: Soils and Plant Nutrition

Piracicaba
2018

Dados Internacionais de Catalogação na Publicação

DIVISÃO DE BIBLIOTECA – DIBD/ESALQ/USP

Piccolla, Cristiano Dela

Use of bone char and biochar for recycling phosphorus into agricultural systems / Cristiano Dela Piccolla. - - versão revisada de acordo com a resolução CoPGr 6018 de 2011. - - Piracicaba, 2018.

77 p.

Tese (Doutorado) - - USP / Escola Superior de Agricultura “Luiz de Queiroz”.

1. Fertilizante fosfatado alternativo 2. Germinação de esporos de FMA 3. Solos tropicais 4. Fertilizante alternativo I. Título

Aos meus avós João e ***Laura, Pedro e Nair (in memoriam),***

por terem sido exemplos de humildade, honestidade e caráter

Aos meus pais, Clovis e Leonice e irmão Leandro,

Pela união e apoio mútuo em todos os momentos

Dedico

À Thalita e aos grandes amigos,

pelo companheirismo, respeito e cumplicidade

Ofereço

ACKNOWLEDGMENTS

I thank God for the grace of life. I thank my parents Clovis and Leonice and brother Leandro for always supporting me. I specially thank Thalita Cardoso Anastácio, a very special girl I had the opportunity to meet and who made me feel full of life. She supported me in crucial moments during my doctorate. I thank my extended family for the unity and all the good moments we spent together. I specially thank my advisor Dr. Takashi Muraoka for his supervision and friendship and my co-advisor Dr. Etelvino Henrique Novotny for his guidance, friendship, and the great opportunities at working in partnership with international groups he provided me. I thank Dr. Dean Hesterberg for being so kind, helpful and for teaching me special things at North Carolina State University, which made my time in US very productive. I thank Dr. Masanori Saito for receiving me as a trainee in his laboratory in Kawatabi Field Center, Japan. The time I worked under his supervision and the experiences I had with my Japanese friends was unforgettable and contributed a lot to amplify my knowledge and cultural baggage. I thank Soils and Plant Nutrition Graduate Program and Center of Nuclear Energy in Agriculture of University of Sao Paulo where I studied and carried out my experiments. I specially thank my friend and colleague Josimar for being so kind and helpful always he could. I also thank all my friends from Soil Fertility Laboratory and the ones I met in Piracicaba. I specially thank my great friends Leandro Almeida, Luiz Ricardo Nakamura, Alan Winkler, Bruno Marçal de Almeida, Mauricio Rodrigues and Wagner Wolf for all good moments and experiences we had together. I thank the Professors Dr. Alvaro Mafra and Dr. Ildegardis Bertol who firstly immersed me into the scientific life. I also thank Professor Dr. Marcelo Alves for his friendship, guidance and help in my experiments. I thank Capes and CNPq for providing scholarships that allowed me to satisfactory accomplish undergraduate and graduate degrees.

HEADING

“A nobreza da árvore não é comparada pelas tempestades que suportou, mas pelos frutos que apresentou”

João Expedito Franco

CONTENTS

RESUMO **8**

ABSTRACT **9**

1. IMPROVING BONE-BASED PHOSPHATE FERTILIZER BY PYROLYSIS 11

Abstract 11

1.1. Introduction 12

1.2. Material and Methods 14

1.3. Results 17

1.4. Discussion 25

1.5. Conclusion 29

References 29

Supporting information 33

2. PYROLYSIS AS ALTERNATIVE TO CALCINATION FOR BONE-BASED FERTILIZER GENERATION 39

Abstract 39

2.1. Introduction 40

2.2. Material and Methods 41

2.2.1. Bone char P release kinetics 41

2.2.2. Plant ^{32}P uptake from fertilizers 42

2.3. Results and Discussion 45

2.3.1. Bone char P release kinetics 45

2.3.2. Plant ^{32}P uptake from fertilizers 47

2.4. Conclusion 50

References 51

3. BIOCHAR AS A TOOL TO ENHANCE PLANT GROWTH IN A SOIL WITH LOW PHOSPHORUS CONTENT: THE SYMBIOTIC PATHWAY 53

Abstract 53

3.1. Introduction 54

3.2. Material and Methods 56

3.2.1. Biomass pyrolysis 56

3.2.2. Biochar characterization 56

3.2.3. Arbuscular mycorrhizal fungi spore germination 56

3.2.4. Growth and nutrient uptake of plants submitted to biochar and AMF inoculation 58

3.3. Results and Discussion 60

3.3.1. Pyrolysis products yield and biochar characteristics 60

3.3.2. Arbuscular mycorrhizal fungi spore germination 63
3.3.3. Growth and nutrient uptake of plants submitted to biochar and AMF inoculation ... 64
3.4. Conclusion 71
References 72
Supporting information 75
FINAL CONSIDERATIONS 77

RESUMO

Uso de carvão de osso e biocarvão para reciclagem de fósforo em sistemas agrícolas

O fósforo (P) é um macronutriente para as plantas e solos localizados em regiões tropicais geralmente apresentam baixo conteúdo deste elemento. Ainda, estes solos são ácidos e apresentam alta capacidade de fixação de P, diminuindo substancialmente a eficiência de fertilizantes. Por esta razão, adições anuais de P ao solo são requeridas para obtenção de produtividades de plantas economicamente viáveis. A principal preocupação em relação ao uso de P na agricultura é que este elemento é extraído de minas que estão sendo exauridas. Por esta razão, é necessário o desenvolvimento de tecnologias de reciclagem de P a fim de economizar recursos minerais e obter benefícios oriundos de fontes de baixo custo disponíveis localmente. Um material que é rico em P e que poderia ser empregado na reciclagem de fósforo é o osso animal, no entanto, este subproduto da indústria de carnes necessita ser tratado previamente ao uso para garantir segurança sanitária. A pirólise é umas tecnologias que tem recebido atenção porque seu emprego no tratamento de ossos não afeta a estrutura do material como a calcinação, que é um tratamento padrão. Realizar a pirólise de ossos gera um material denominado de carvão de osso (*bone char***,** em inglês), o qual testes sugerem que a sua eficiência é comparável à fertilizantes solúveis convencionais obtidos a partir de rochas fosfáticas. Outra forma de obter maior absorção de P e nutrientes e maior produtividade de cultivos é através do estímulo da simbiose de plantas com micorrízicos arbusculares (FMA), estes naturalmente encontrados em solos. No entanto, solos ácidos de regiões tropicais geralmente dificultam a interação de plantas-FMA devido ao elevado teor de alumínio trocável presente. Uma alternativa para superar esse problema seria a aplicação de pirólise a resíduos orgânicos, gerando assim um material chamado biocarvão, o qual é rico em carbono, e as vezes nutrientes, e poderia auxiliar na simbiose de plantas com AMF. Nosso objetivo foi produzir através da pirólise um conjunto de biocarvões em diferentes temperaturas (400, 550 e 800 °C) e composições atmosférias (câmara selada, fluxo de N_2 e fluxo de vapor d'água) e realizar a caracterização dos materiais resultantes (capítulo 1) para verificar que possíveis fatores controlam a eficiência do carvão de osso em um experimento em vasos com marcação com ^{32}P (capítulo 2). A fim de testar o viés simbiótico na aquisição de P pelas plantas com o uso de biocarvão, dois biocarvões de cavaco de eucalipto produzidos a 300 e 700 °C foram aplicados a um solo inoculado ou não com FMA (capítulo 3). Nesse experimento foram analizados o crescimento de plantas e colonização por FMA, como também a absorção de nutrientes. Adicionalmente, um teste com a germinação de esporos de FMA foi realizado para investiar possíveis effeitos positions ou inibitórios dos biochar em esporos de FMA.

Palavras-chave: Reciclagem de fósforo; Tratamento de ossos; XANES.

ABSTRACT

Use of bone char and biochar for recycling phosphorus into agricultural systems

Phosphorus (P) is a plant macronutrient and soils located in tropical regions generally show low content of this element. Moreover, these soils are acidic and show high fixing capacity of phosphorus, substantially decreasing fertilizers efficiency. For this reason, annual P inputs to soils are required to obtain feasible crop yields. The main concern regarding P in agriculture is this element is extracted from mines that are being depleted. For this reason, it is necessary to develop recycling P technologies in order economize mineral resources and obtain benefits from low cost sources locally available. Bones are a P-rich material that could be employed for P recycling; however, this sub-product from meat industry needs to be treated prior use to ensure health safety. Pyrolysis is a technology that has gained attention because it does not affect bone mineral structure as does calcination, which is a standard treatment. Performing pyrolysis of bones generates a material called bone char and tests suggests that its efficiency is comparable to common soluble fertilizers obtained from P rocks. Another way to obtain higher crop P and other nutrients absorption as well as yield, is to stimulate symbiosis of plants with arbuscular mycorrhizal fungi (AMF), which are naturally found in soils. However, acidic soils from tropical regions generally difficult plant-AMF interaction due to high amount of exchangeable aluminum present. An alternative to overcome this issue would be to apply pyrolysis to organic wastes, generating a material termed biochar, which is rich in carbon, and sometimes nutrients, assisting AMF-plant symbiosis. Our aim was to produce through pyrolysis a set of bone chars in different temperatures (400, 550 and 800 °C) and atmospheric composition (sealed chamber, N_2 flux and steam flux), and perform a detailed characterization of the resultant materials (chapter 1) to verify which possible factors are controlling bone char efficiency as fertilizer in a pot experiment labelled with ^{32}P (chapter 2). To test the symbiotic pathway in P acquisition by plants through biochar use, two biochars from eucalyptus wood chips were produced at 300 and 700 °C and applied to a soil inoculated or non-inoculated with AMF. In this experiment we analyzed plant growth and colonization by AMF as well as nutrient absorption (chapter 3). Additionally, a trial with AMF spore germination evaluation was performed to investigate the possible inhibitory or positive effects of the biochars on AMF fungi.

Keywords: Bone treatment; Phosphorus recycling; XANES.

1. IMPROVING BONE-BASED PHOSPHATE FERTILIZER BY PYROLYSIS

Abstract

The projected long-term scarcity of phosphorus for food production underlies a need for more efficient P recycling technologies. Our objective was to determine the effects of various pyrolysis treatments on the mineralogy and solubility of P in bones. We analysed selected physical, mineralogical, and chemical characteristics of P in bone chars produced by pyrolyzing swine bones at 400, 550 or 800 °C in a sealed chamber, under N_2 gas, or by steam activation. X-ray diffraction (XRD) and synchrotron X-ray absorption near edge structure (XANES) spectroscopy at P and Ca edges showed that bone chars were all composed of hydroxyapatite (HAP). However, pyrolysis in a sealed chamber or under $N_{2(g)}$ diminished HAP crystallinity compared with pyrolysis with steam activation or calcination at 800 °C. Pyrolysis in a sealed chamber at 550 and 800 °C showed greater total and citric-acid-soluble P contents compared to the other treatments, in part due to loss of combustible organics. Our results indicate that pyrolysis is an effective treatment for converting animal-bone waste into an effective fertilizer that can recycle P back into agriculture systems.

Keywords: Alternative phosphate fertilizer; Bioapatite; Bone treatment.

1.1. Introduction

Phosphorus is essential for life and a lack of plant-available P in soils worldwide is of concern for long-term food security (VAN VUUREN; BOUWMAN; BEUSEN, 2010; CORDELL, 2017). In agricultural systems, soils are amended with phosphate fertilizers to sustain optimal crop yields. However, future population growth and the economic rise of developing countries that presently use less than optimal fertilizer inputs could remarkably increase P mineral demand. Particularly in tropical regions, high P inputs to soils are needed because the highly weathered soils, naturally poor in P, contain also more abundant Fe and Al oxide minerals that can fix applied P, thereby resulting in fertilization efficiencies generally <20% (MAHISARAKUL et al., 2002).

Most countries import phosphate-fertilizer resources. Commonly used fertilizers include sedimentary rocks that are extracted from mines or belowground for direct field application, and water-soluble phosphate compounds produced by treating igneous rocks with acids. Eighty eight percent of world's primary P reserves are controlled by only five countries, and Morocco alone controls 75% of the P reserves, part of which are located in a territory disputed with Western Sahara (CORDELL, 2017). Morocco's territorial occupation and resource exploration in Western Sahara by Morocco has persisted for 43 years, mainly due to the presence of phosphate rock mines. Geopolitical crises in such regions could trigger phosphate shortages (SMITH, 2015). Shortages and overall depletion of primary P reserves can be delayed by seeking alternative P sources, recycling and/or recovering P from wastes, and improving soil P management.

Bones are a waste product of the meat industry that can potentially serve as an alternative source for agricultural P. These bones are now mostly used in animal feeds. However, if not treated correctly to destroy disease sources, they can cause health and environmental issues. As a result, feeding bone meal to farm animals has been has been banned in the European Union since 2001 and in Brazil only bones treated through calcination (process explained below) are allowed in bovine feeds. For example, bone (and animal protein) meals were blamed for the spread of BSE (bovine spongiform encephalopathy, also called "mad cow disease") that hit Great Britain and the rest of Europe, with respectively 184,600 and 5,250 cases in bovines confirmed by 2007 following its discovering in 1985 (EU FOOD SAFETY, 2007). Estimated BSE-related economic losses were £3.7 billion (THE INDEPENDENT, 2000) and the variant Creutzfeldt-Jakob disease (vCJD) was responsible for 224 human deaths worldwide (BERTOLINI, CURLING, GOSS, 2013), mostly in Great Britain. Bone treatments

that have been designed to eliminate BSE disease sources might also be viable for producing bone-based phosphate fertilizers as an alternative use for this waste product.

The inorganic matrix of bone is primarily composed of poorly crystalline hydroxyapatite (HAP) containing structural carbonate (CO_3^{2-}), which substitutes for hydroxyls or phosphates and increases the solubility of bone HAP compared with pure HAP (ITO et al., 1997; REY et al., 2009). Once still there are no specific regulations about presence of disease sources in bones designated to be used as fertilizer, an ideal bone treatment for fertilizer production would have to eliminate potential disease sources and increase the solubility of the bone mineral structure, e.g., by inhibiting HAP crystallization. Examples of common treatments that do not employ chemical reagents are steaming, autoclaving, and calcination. Even research on this topic is not extensive, calcination is effective at eliminating destroying both microorganisms and prions (protease-resistant proteins responsible for BSE) (BROWN et al., 2004). However, the high temperatures employed (700 to >1200 °C) generally volatilize most organic compounds (FIGUEIREDO et al., 2010; KHOO et al., 2015), and change the structure of bone HAP. On the contrary, steaming and autoclaving at lower temperatures (100-121 °C) might minimize changes in bone HAP structure, but are not sufficient to denature prions (TAYLOR et al., 1994). Pyrolysis is an alternative thermal treatment that employs temperatures as high as those used for calcination, but the absence of O_2 causes only partial decomposition of organics in the bone, resulting in a material called *bone char*. However, the temperature of pyrolysis needed to denature prions still needs to be tested, once it could largely vary (~400 to >1000 °C). Activation steps such as a flux of inert gas (e.g. N_2) during pyrolysis are widely employed in activated carbon production and could be used to enhance bone-char surface area and solubility (IOANNIDOU; ZABANIOTOU, 2007).

To optimize treatments for converting animal-bone waste into efficient phosphate fertilizer materials, it is important to understand how the mineralogical, physical, and chemical properties of bone changes under different pyrolysis conditions. Thus, we hypothesize that pyrolysis generates a more soluble material than calcination and activation steps enhance physical properties (porosity, surface area) of bone chars towards solubility. Our objective was to determine the effects of various pyrolysis temperatures and activation-gas treatments on properties of bone chars that affect P solubility and the potential suitability of these materials as an agricultural fertilizer source.

1.2. Material and Methods

Femur and scapula bones of ~130 day-old swines weighing ~100 kg were collected from a butchery and subjected to pyrolysis in a chamber of 60 L, which was composed of AISI (American Iron and Steel Institute) type 304 stainless steel. Pyrolysis was performed at 400, 550 and 800 °C in a sealed chamber (oxygen depleted atmosphere). The chamber body was composed of. To determine the relevance of activation during pyrolysis on specific surface, porosity, and P solubility; additional samples were heated to 550 and 800 °C under a flux of nitrogen gas (N_2) (10 L min^{-1}) and steam/water vapor (WV) was used as a low-cost alternative and applied to samples heated to 800 °C. The steam contained dissolved O_2, and the flow was not measured. Bone calcined at 800 °C in an open atmosphere (CA treatment) served as a control. A heating rate of 40 °C min^{-1} with 30 minutes of residence time at the treatment temperature was applied to all samples. Femoral bone from an ~150 day-old animal was collected, washed with boiling water, dried for 5 days at 65 °C and used as a standard for X-ray diffraction (XRD) and X-ray near-edge absorption spectroscopy (XANES) data interpretation. Yields of bone chars produced at 400 °C in sealed chamber, 800 °C under steam activation, and calcined bones, were calculated by mass balance before and after treatments. All samples were finely ground by hand with an agate mortar and pestle for further analyses.

Synchrotron XRD analysis was performed at the XRD1 beamline of the Brazilian Synchrotron Light Laboratory (LNLS – Campinas, Sao Paulo State, Brazil). The beamline apparatus and analysis conditions were described by Carvalho et al. (2016). Finely powdered bone char samples and three standard HAPs (reagent grade; reagent grade nano-sized; and synthesized at 90 °C) were introduced in capillary tubes (Ø=0.3 mm) and analyzed for 240 seconds using an X-ray beam energy of 12 keV. Minerals were identified using the JCPDS powder diffraction search manuals after setting and subtracting a baseline (sp-line) from the diffractograms. Crystallite sizes of minerals were estimated using the Debye-Scherrer equation with a shape factor (K) of 0.9. Full widths at half-maximum (FWHM) (values shown in Table S1.1) were calculated using the Origin® plotting software after fitting a Voigt profile to the 002 diffraction peak, the only non-overlapping peak present in all of our samples (PATEL et al., 2015). The estimated crystallite sizes are considered minimal values because instrumental broadening and structural micro-deformations were not considered.

XANES spectra were acquired at the P and Ca K and L-edges to assess the presence of amorphous calcium phosphates (P-Ca) and any compounds that were not detected by XRD analysis

XANES spectra at the Ca and P K-edges at ~4039 and ~2151 eV, respectively, were collected at the Soft X-ray Spectroscopy (SXS) beamline at LNLS using a Si(111) double crystal monochromator. Finely powdered samples were diluted in boron nitride (BN) to a Ca or P concentration of <2% (w/w) to diminish self-absorption. A thin layer of this mixture was spread onto double-sided carbon tape affixed to and aluminum multiple-sample holder. Fluorescence-mode data were collected under vacuum at ~10^{-7} mbar, and at least triplicate scans were obtained from each sample positioned at 45° angle relative to both the incident beam and detector to decrease elastic scattering. Data were collected over energy ranges of 2120 to 2300 eV for P and from 4000 to 4200 eV for Ca K-edge XANES. Energy step sizes and other data-collection parameters are shown in Table S1.2. A calcium-phosphate standard was used for energy calibration at the P edge, with E0 set at 2150.7 eV for the maximum in the first derivative. The same standard and calibration procedure was used for Ca K-edge XANES. The Athena® data analysis software (RAVEL; NEWVILLE, 2005) was used to merge replicated spectra, subtract a baseline using a linear regression model fit across an energy range between -40 and -12 eV relative to E0, and normalize spectra using a linear regression across a relative energy region between 65 and 150 eV, for Ca K-edge. For P K-edge spectra the baseline was subtracted utilizing linear regression model fits that best represented the pre- and post-edge regions of the spectra. The flatten mode in Athena was used to produce normalized XANES spectra.

The proportions of spectra for Ca standards (Fig. S1.3) that gave the best fits to Ca K-edge spectra of bone char samples were determined using linear combination fitting (LCF) analysis, following the standard-elimination procedure described by Manceau (MANCEAU; MARCUS; GRANGEON, 2012). Fitting was performed only for Ca K-edge spectra over an energy range between -11 and 65 eV relative to E0. An amorphous calcium phosphate (ACP) (Sigma-Aldrich®) standard and reagent grade HAP was utilized to model the extent of changes in mineral ordering under our various heat treatments. Although a review of bone mineralogy (REY et al., 2009) indicated that ACP was not present, the Ca K-edge XANES spectrum of our ACP was similar to (and representative of) the spectrum of poorly crystalline HAP as reported by Oxmann (2014).

Spectra of $L_{II,III}$-edge XANES were acquired at the Planar Grating Monochromator (PGM) beamline at LNLS (CEZAR et al., 2013). Samples and standards were prepared similarly to those for K-edge spectroscopy. The beamline energy was calibrated with copper oxide at 930 eV, which is ~582 and 795 eV above the reported Ca and P L_{III}-edges, respectively. The energy calibration was then checked at the Ca and P edges (348.6 and 137.2 eV) using

HAP. Measurements were carried out at ambient temperature under vacuum (10^{-11} bar), and the planar grating monochromator had a spectral resolution of ~0.02 eV. Spectra were acquired from 130 to 160 eV for P and 343 to 357 eV for Ca, with fixed step sizes of 0.05 and 0.075 eV, respectively. The standards used for both elements are listed in Table S1.3 and shown in Figs. S1.4 and S1.5. Spectra were first baseline subtracted using a linear fit to the pre-edge. The following double arctan function was then fit across each spectrum:

$$f(\Delta E) = \frac{h_1}{\pi}\left[\arctan\left(\frac{\pi}{w_1}(\Delta E - E_1)\right) + \frac{\pi}{2}\right] + \frac{h_2}{\pi}\left[\arctan\left(\frac{\pi}{w_2}(\Delta E - E_2)\right) + \frac{\pi}{2}\right] \quad (1)$$

The fitted arctan functions were subtracted from spectra to correct the anomalous behavior of Ca and P $L_{II,III}$-edge spectra (example shown in Fig. S1.1) (BOURDELLE et al., 2013; COSMIDIS et al., 2015). Spectra were then normalized to unit vector length in Matlab®, and the edge position was set as the zero crossing of the second derivative. Because of the high sensitivity of $L_{II,III}$-edge spectra for different Ca-phosphates, we qualitatively compared diagnostic spectral features of standards with those of bone chars to try to identify minor phases that were not detected by XRD. Partial-spectra LCF analyses were also performed in several different regions of our spectra (one at a time) to corroborate species determined by K-edge XANES and XRD analyses.

Specific surface areas, pore volumes, and pore diameters of bone chars were determined by the multi-point Brunauer–Emmett–Teller (BET) method described in Schimmelpfennig and Glaser (2012) using a Quantachrome Model Nova 2000e analyzer. Samples were heated at 150 °C for 3 h prior to analysis. pH was measured in deionized water 1:20 (m:v) after shaking for 90 minutes (RAJKOVICH et al., 2012). Carbon, nitrogen and hydrogen were determined by combustion of chars using a LECO analyzer and nutrients, heavy metals and other elements (Ba, Na, Si) were analyzed by ICP-OES after digesting samples by a modified dry-ash method (ENDERS; LEHMANN, 2012).

Phosphate soluble in water (P_w), neutral ammonium citrate (P_{NAC}), and 2% citric acid (P_{CA}) were measured (AOAC, 1999) as alternative predictors of P availability from fertilizers. The 2% citric-acid extraction is commonly used to determine plant available P from low-soluble fertilizer sources such as rock phosphate. The proportion of 2% citric-acid soluble P relative to total P in bone chars was used to compare bone chars on an equivalent basis.

Co-dependence of bone-char physical and chemical properties were assessed using regression analysis, with goodness of fits and confidence intervals calculated in SAS®.

1.3. Results

Mass loss during heating decreased the yield of bone chars products relative to the original, non-treated bones. Bones subjected to pyrolysis at 400 °C in a sealed chamber yielded 50% (w/w) bone char, whereas steam-activated and calcined bone, both produced at 800 °C, had yields of 36 and 30%, respectively. Because loss of C drives bone char yield in the temperature range of our experiments, other samples were considered to have intermediary yields.

X-ray diffraction patterns for all standards and treated bone samples show a dominance of hydroxyapatite of varying crystallinities, except for a minor 012 peak for calcite was detected at 3.86 Å in the calcined bone sample (partial data shown in Fig. 1.1A and B). For nano-sized and synthetic HAP standards, all XRD peaks reported in JCPDS powder diffraction card 9-432 out to 100 °2-theta were present in our patterns. Less crystalline bone char samples showed XRD patterns consistent with our crystalline HAP standard, except for some minor peaks reported for HAP were not detectable due to peak broadening. Peaks at 21-21.5 °2–theta that are labeled as Miller indices 211 and 112 can be overlapping peaks from hydroxyapatite and calcite, suggesting that the bone hydroxyapatites contained structural carbonates. After calcination and steam activation at 800 °C these peaks became more well-defined, indicating crystallization (LANDI et al., 2003).

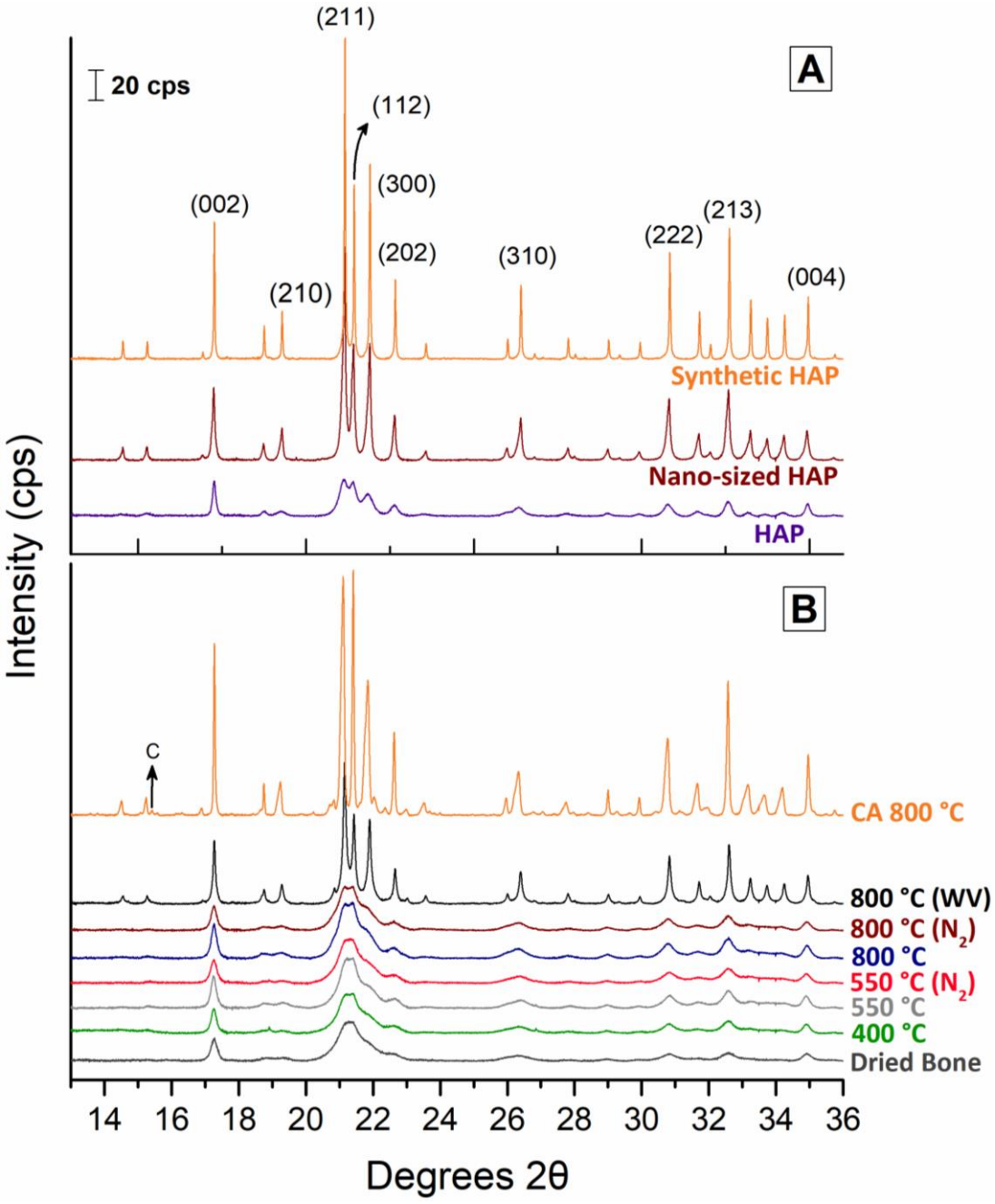

Figure 1.1 X-ray diffraction patterns of hydroxyapatite (HAP) standards (plot A); and dry swine bone (for reference), bone chars produced under different conditions, and calcined (CA) bone sample (plot B). A minor 012 peak for calcite is labeled "C".

Phosphorus and calcium K-edge XANES spectra also showed a dominance of HAP in bone-char samples. For example, shoulders at 2154 and 4055 eV and a peak at 2162 eV in spectra for HAP were less prominent in the spectrum for ACP (Fig. 1.2A, B). However, LCF results of Ca K-edge XANES spectra showed a decreasing proportion of ACP relative to HAP with increasing treatment temperature, ranging from 20% ACP for the 400 °C sealed-chamber treatment to a non-detectable level at 800 °C for the steam-activated treatment (Table 1.1).

Although spectrum of calcined bone was not obtained for Ca K-edge, due its similarity with the steam-activated sample, it is not expected detectable levels of ACP compounds in this sample.

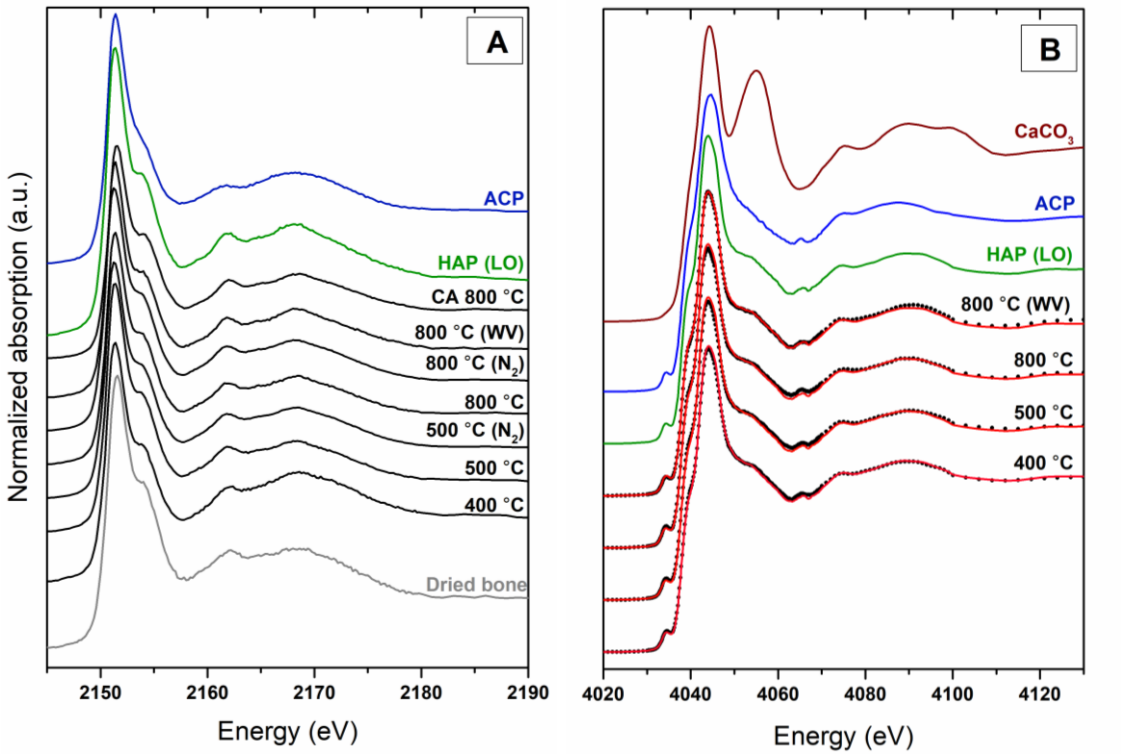

Figure 1.2 Phosphorus (A) and calcium (B) K-edge XANES spectra of standard compounds and bone chars produced at different temperatures and atmosphere compositions. Black dots and red lines in B are respectively the data and overlaid linear combination fits. ACP: amorphous calcium phosphate; HAP: hydroxyapatite; CA: calcined bone; LO: low-ordered (reagent grade HAP); WV: steam-activated; N_2: nitrogen-activated. Samples with no parentheses after temperature labels were produced in sealed chamber with no flux of gases.

Table 1.1 Linear combination fitting (LCF) results showing proportions (%) of standards giving the best fit to Ca K-edge XANES spectra of bone char samples †

Bone char	HAP	ACP	Goodness of fit
	(%)		(R-factor)
BC 400 °C	80	20	0.0007
BC 550 °C	84	16	0.0016
BC 800 °C	89	11	0.0014
BC 800 °C (WV)	100	-	0.0004

† BC: bone char; HAP: hydroxyapatite (low ordered); ACP: amorphous calcium phosphate; WV: steam-activated bone char.
R-factor = ∑ (data – fit)/ ∑ (data)

Consistent with XRD and K-edge XANES results, P $L_{II,III}$-edge XANES spectra from bone char samples revealed similar features of samples to that of low ordered HAP (Fig. 1.3A). In addition, calcined sample (800 °C) showed unique spectral features, with stronger peaks than bone char samples at energies ranging from 136 to 140 eV and 147 eV, which were more consistent with our highly ordered HAP. Linear combination fitting performed from -0.3 to 2.7 eV relative to E0 pointed out no presence of compounds other than HAP in bone char, although data for the ACP standard were not available for fitting (see standard list in SI). In addition, Ca $L_{II,III}$-edge XANES spectra showed no evidence for calcite or calcium oxide, which showed a stronger peak near 351 eV (Fig. 1.3B). Carbonates represent 3-6 wt% of bones and are generally present in calcite form or integrated into HAP structure (MAYER; FEATHERSTONE, 2000; REY et al., 2009). This proportion of carbonates might be below detection by Ca $L_{II,III}$-edge XANES, although other researchers found $CaCO_3$ by peak shifting in bone char spectra (RAJENDRAN; GIALANELLA; ASWATH, 2013).

Physical properties of the heated bone samples varied between some treatments (Table 1.2). Crystallite sizes determined from XRD suggested that heating samples between 400 and 800 °C in the absence of O_2 inhibited crystallization of HAP. For example, nearly all bone char samples had crystallite sizes between 24 and 29 nm, whereas that of the calcined control sample was 112 nm. The bone char sample activated with water vapor containing dissolved O_2 while heating to 800 °C had an intermediate crystallite size of 65 nm. Measured pore volumes tended to decrease with increasing crystallite size, as the structure becomes more ordered, except that the 400 °C sample had an 8- to 16-fold lower pore volume than the other charred samples. We believe this difference is due to condensation of volatilized organic compounds in smaller pores (NOVOTNY et al., 2015), as indicated by its greater C and H contents and pore diameter (Table 1.2 and 1.3). Activating bone chars and calcination of bones reduced 18% of pore diameter compared with samples treated in a sealed chamber, and specific surface trended with pore volume.

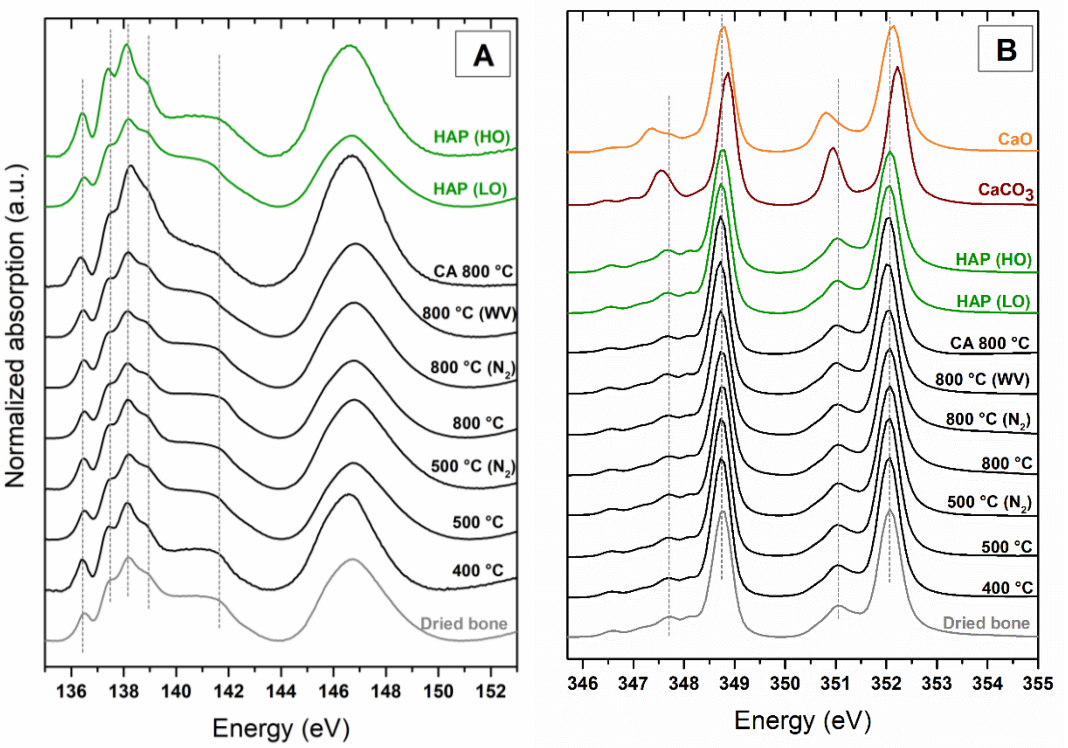

Figure 1.3 Phosphorus (A) and calcium (B) $L_{II,III}$-edge XANES spectra of standard compounds and bone chars obtained under different temperatures and atmosphere compositions. HO: highly ordered (synthetic HAP); LO: low ordered (reagent grade HAP). WV: steam activated; N_2: nitrogen activated. Samples with no parenthesis after the temperature were produced in sealed chamber with no gas flux. Dotted vertical lines support peak position visualization.

Table 1.2 Crystallite size and physical properties of hydroxyapatites, bone materials and bone chars produced under different temperatures and atmosphere compositions

Bone treatment	Crystallite Size (nm)	Pore Volume ($cm^3\ g^{-1}$)	Pore Diameter (Å)	SA ($m^2\ g^{-1}$)
Dried bone	23	-	-	-
BC 400 °C	29	0.01	42	3
BC 550 °C	29	0.15	35	87
BC 550 °C (N_2)	24	0.15	33	88
BC 800 °C	28	0.16	35	89
BC 800 °C (N_2)	26	0.16	32	101
BC 800 °C (WV)	65	0.08	30	53
CA 800 °C	112	0.01	28	5
Hydroxyapatites				
HAP[a]	47	-	-	-
Nano-sized HAP[b]	66	-	-	>9.4[d]
Synthetic HAP[c]	152	-	-	-

SA: surface area; BC: Bone char; CA: calcination; N_2: activated by nitrogen gas flux; WV: activated by steam/water vapor; HAP: hydroxyapatite.
[a] Reagent grade
[b] Particle size: <200 nm
[c] Laboratory synthesized at 90 °C
[d] Value from Sigma-Aldrich

Table 1.3 Carbon, hydrogen, nitrogen, C:N ratio and pH of calcined bones and bone chars produced by pyrolysis under different temperatures and atmosphere compositions

Bone treatment	Carbon (%)	Hydrogen (%)	Nitrogen (%)	C:N	pH
BC 400 °C	29	3	4	7.25	7.7
BC 550 °C	17	1	3	5.7	8.3
BC 550 °C (N_2)	19	1	3	6.3	8.5
BC 800 °C	18	0.7	2	9	9.3
BC 800 °C (N_2)	18	0.7	2	9	9.2
BC 800 °C (WV)	11	-	1	11	9.9
CA 800 °C	0.8	-	0.4	2	10.1

BC: bone char; CA: calcined bone; N_2: activated by N_2 flux; WV: activated by steam

Carbon, hydrogen and nitrogen content decreased with temperature increase. Bone char 400 °C had around 10% more carbon than the other bone materials, except for the steam-activated and calcined treatments that were, and 10 times more nitrogen than calcined bone (Table 1.3). Calcination and activation with steam, both containing reactive oxygen, resulted in an augmented loss of organic compounds. Bone chars had low C:N ratio (≤11) when compared with reported values for plant materials and biochars (KLOSS et al., 2012). Calcined bone showed the lowest value, which was 5.5-fold lower than steam-activated treatment.

The pH of the produced bone materials ranged from 7.7 in 400 ° C bone char to 10.1 in calcined sample and trended with pyrolysis temperature and organic compounds loss (Table 1.3). As organic compounds were volatilized during pyrolysis, elements with higher thermal

stability (e.g. Mg, K and Na) were likely accumulated as oxides, which confer a basic character of their hydrolysis products (Table 1.4 and 1.5). Sobczak-Kupiec; Wzorek, (2012) showed that the decomposition of bone hydroxyapatite carbonates generated calcium oxide, but the CaO formed was increased only above 750 °C.

Total P content on a P_2O_5 basis (P_T-P_2O_5) varied from 31.6% in 400 °C bone char to 60.7% in calcined bones (Table 1.4). These values are greater than the average (27%) of a set of 25 phosphate rocks found around the world (TRUONG; ZAPATA, 2002). All bone chars meet the minimum amount of 20% of P_2O_5 to be considered economically viable. Moreover, they meet the European Council regulations for P rock commercialization that requires a minimum of 12% of P_2O_5 (EC, 2016). Bone chars produced at 550 and 800 °C in the sealed chamber showed the greatest citric-acid-soluble (P_{CA}) and total P (P_T) contents, except for the steam-activated bone char that had greater P_T content. The relative amount of P_T soluble in citric acid (P_{CA}/P_T) indicates the bone char P fraction that is potentially available to plants. All bone chars P_{CA}/P_T ranged from 42% in steam-activated bone char to 63% in the N_2-activated sample produced at 550 °C, which were greater than the rock phosphates evaluated by Truong and Zapata (2002). Bone char produced at 400 °C in the sealed chamber showed similar P_{CA}/P_T compared to steam-activated sample, while other bone chars had higher values. The 800 °C-calcined bone sample, which also contained the most crystalline HAP, had the lowest P_{CA}/P_T (26%), which was 2.4-fold lower than the most soluble bone char [BC 550 °C (N_2)]. Phosphorus soluble in water (P_w) and neutral ammonium citrate (P_{NAC}) represented a small fraction of the P_T content in bone chars, with a maximum of 0.8% of P_{NAC} in bone chars produced at 550 and 800 °C in sealed chamber. Therefore, bone chars should be highly dependent on soil acidity to dissolve their HAP and release P to plants.

Table 1.4 Total P and Ca, and phosphate dissolved by different extractants from swine bones charred and calcined under different temperatures and atmosphere compositions. The P extracted by 2% citric acid is a metric of plant-available P, whereas water- and neutral ammonium-citrate-extractable P reflects relative P solubility at the pH of the samples or by complexometric dissolution

Bone treatment	P_w	P_{NAC}	P_{CA}	P_T	P_T-P_2O_5	P_{CA}/P_T	Ca
	%	%	%	%	%	%	%
BC 400 °C	0.00	0.6	6.0	13.8	31.6	43	20.3
BC 550 °C	0.13	0.8	10.7	20.5	46.9	52	23.6
BC 550 °C (N_2)	0.13	0.5	10.6	16.7	38.2	63	23.7
BC 800 °C	0.09	0.8	11.0	20.6	47.2	53	24.8
BC 800 °C (N_2)	0.08	0.6	9.4	19.0	43.5	50	24.6
BC 800 °C (WV)	0.03	0	8.9	21.1	48.3	42	31.2
CA 800 °C	0.02	0.1	6.9	26.5	60.7	26	32.6

P_w: water-extractable phosphorus; P_{NAC}: neutral ammonium citrate-extractable P; P_{CA}: 2% citric-acid-soluble P; P_T: total P; P_T-P_2O_5: total P in P_2O_5 basis; P_{CA}/P_T: proportion of total P that is soluble in citric acid; BC: bone char; CA: calcination; N_2: activated by nitrogen gas flux; WV: steam activation

Bone chars also contained around 0.5-1% of magnesium and potassium, which are plant macronutrients and minor amounts of the micronutrients Zn, Fe, Cu and Ni. Steam activation and calcination, both at 800 °C, remarkably increased Fe, B, Cu, Mn and Ni contents (Table 1.5), apparently due to loss of sample mass (e.g., organic and inorganic C) during heating. Cadmium, a common toxic heavy metal, increased in the samples from 2.2 to 3.9 mg kg^{-1} with increasing treatment temperature, but was always at least 15-fold below the European limit of 60 mg kg^{-1} P_2O_5 for inorganic fertilizers (EC, 2016). Calcined bone had a Ni content of 164 mg kg^{-1} and was the only sample that exceeded the European Ni limit of 50 mg kg^{-1}. We attributed the mass loss during calcination the responsible for such high Ni content values once there was no abrasion between pyrolysis chamber and bone char, eliminating the possibility of sample contamination. Limits adopted in Europe are referenced here because they are the most restrictive compared to Brazil and some other countries (e.g. Japan, Australia, USA, Canada).

Table 1.5 Elemental content of bone chars produced by pyrolysis in sealed (oxygen depleted) or activated with nitrogen or steam. Calcined bone was used as control.

Bone treatment	Mg	K	Zn	Fe	Na	Al	B	Ba	Cd	Cu	Mn	Ni	SiO_2
	g kg^{-1}					mg kg^{-1}							
BC 400°C	7.0	5.0	0.1	0.2	7.5	40.5	3.6	7.1	2.3	<DL	1.2	1.8	22.7
BC 550°C	10.5	3.7	0.2	0.1	8.5	29.8	3.3	11.2	2.2	<DL	1.0	0.4	14.5
BC 550°C (N_2)	8.5	5.5	0.2	0.3	10.0	42.8	4.0	7.5	2.5	<DL	2.6	1.5	34.9
BC 800°C	8.4	4.3	0.2	0.1	9.3	44.2	3.5	10.9	3.2	<DL	1.7	1.2	27.7
BC 800°C (N_2)	8.6	4.2	0.2	0.2	9.1	31.6	5.9	14.6	2.6	<DL	2.2	1.8	23.6
BC 800°C (WV)	9.9	4.4	0.2	1.5	11.6	54.3	30.3	26.8	3.0	7.9	29.0	38.1	41.4
CA 800°C	11.4	6.0	0.2	5.6	13.5	56.2	11.1	14.8	3.9	27.8	121.7	164.0	34.1

BC: bone char; CA: calcination; N_2: nitrogen activation; WV: activated by steam

1.4. Discussion

Our results showed that bone char is potentially a viable source of plant-available phosphorus derived from waste that could replace a significant amount of high-grade phosphate fertilizer applied in agriculture. Bone chars obtained at 550 and 800 °C in absence of oxygen (sealed chamber or under N_2 flux) had a greater portion of soluble P in general for the three extractants employed (water, neutral ammonium citrate and citric acid). For this reason, once assured that such materials are safe at inactivating BSE sources and eliminating pathogens, such materials would provide an increased amount of P released to the soil. A bone heat treatment of 550 °C under N_2 flux appears to be optimal for plant availability of P as indicated by the fraction of total P soluble in 2% citric acid (P_{CA}/P_T), which was around 10% higher than bones treated at 550 and 800 °C in sealed chamber (Table 1.4). We found a relationship between P_{CA}/P_T and properties of bone char that are related to chemical and physical characteristics.

Both XRD and XANES analysis at the K-edges of Ca and P showed more poorly crystalline HAP in bone chars produced in the absence of oxygen (sealed chamber and N_2 activated) compared to calcined bones and steam activated bone char (Figs. 1.1, 1.2A and B). The first group, except 400 °C-bone char, showed higher P_{CA}/P_T than the latter, mainly because smaller crystallites are more reactive.

The increase in crystallite size for 800 °C-steam activated bone char and calcined bone can be explained by heat induced degradation and volatilization losses of organic compounds, which remarkably decreased from ~30% in 400 °C bone char to less than 1% in the calcined

sample (Table 1.2). All bone chars produced in a sealed chamber and with N_2 activation, which inhibited C loss, had similar crystallite size. Regression analysis suggests that C loss influenced the increase of crystallite size (adj-R^2= 0.95) (Fig. 1.4A) and that such phenomenon had a relationship at diminishing the solubility of bone char (adj-R^2=0.76) (Fig. 1.4C). Therefore, avoiding C losses through pyrolysis in sealed chamber or under N_2 activation would be necessary to inhibit HAP mineral crystallization and create a more soluble fertilizer product. However, animal age/gender (e.g. boar, gilt, piglet) bone type (e.g. femur, ribs, cervical vertebrae) and bone part (e.g. compact bone, spongy bone) would affect bone characteristics such as density, porosity and organic/mineral composition, which could interfere on the extension of pyrolysis and result in contrasting bone char solubility. Carbonate decomposition and dehydroxylation occurs between 700-1350 °C and also contributes to HAP crystallization and porosity reduction, resulting in a more dense and less soluble material (LANDI et al., 2003; HABERKO et al., 2006).

Surface area is mainly a function of porosity and pore diameter, which can vary due to pore blockage or incomplete organic compounds removal, as in the case of 400 °C bone char, and due to crystal growth as occurred in calcined and steam activated samples. In both cases, surface area decreased; however, extractability of P from these samples varied according to crystallite size. Because of different phenomena controlling porosity and surface area in bone chars, such parameters alone are not suitable for predicting the P_{CA}/P_T. For example, bone char produced at 400 °C exhibited an 18-fold lower SA but a P_{CA}/P_T comparable to steam activated bone char, probably due to the increased crystallite size of the latter. However, we argue that chemical extractions might underestimate the real amount of plant available P of 400 °C bone char compared to the amount released in real cultivation conditions because inaccessible bone char surfaces caused by pore blockage with organic deposits might eventually become accessible for reactions after mineral dissolution or organic compounds degradation in soil. Bone char P extractability could vary according with the contact of the extractant solution with mineral surface; nonetheless, crystallinity of HAP seems to be the greatest overall driver o P release across the treatments. Activation steps during pyrolysis were not efficiency at increasing bone char surface area and porosity as first hypothesized. Only minor differences in pore diameters in sealed chamber and N_2-activated bone chars were verified and seems to be determined respectively by condensation and expulsion of volatiles, whereas the lower pore diameter in steam activated and calcined samples we attributed to crystallite growth.

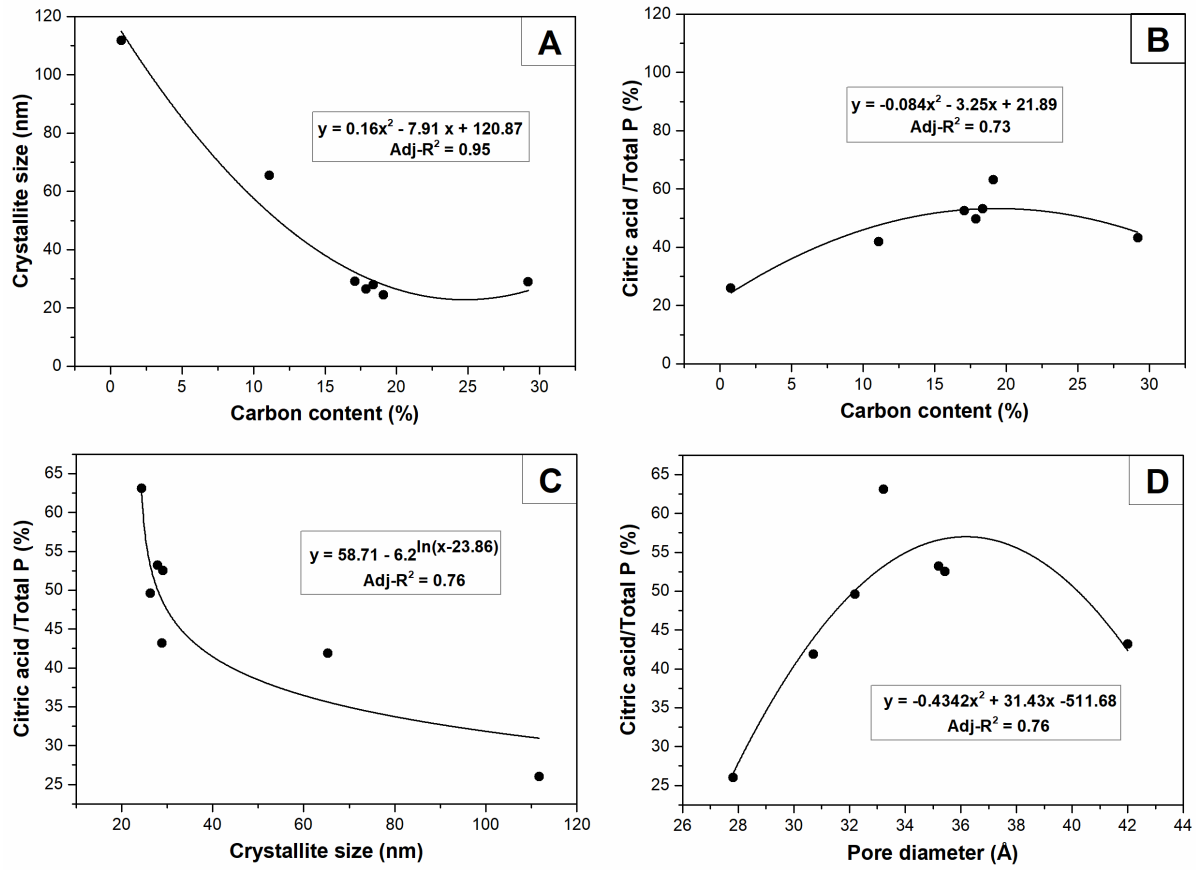

Figure 1.4 Relationships between chemical and physical characteristics of the tested charred and calcined bones.

Considering plant-availability of P as inferred from chemical extractions such as P_{CA}/P_T, producing improved bone-based fertilizers requires high enough temperatures (550 °C) to prevent pore trapping by volatiles. On the other hand, we do not recommend to treat swine bones by pyrolysis at 800 °C with steam activation or calcination (open atmosphere) because the increased hydroxyapatite crystallization results in lower P_{CA}/P_T. We suggest that this metric of plant-available P in bone chars predicted from either specific surface area or carbon content (Fig. 1.4B, D adj-R^2=0.73 - 0.76) as well as crystallite size calculated from XRD data (Fig. 1.4C, adj-R^2=0.76) could help at explaining bone char dissolution behavior and be employed to improve its production technology.

Bone chars produced at 400 and 550 °C could be more cost-effective than materials obtained at higher temperatures. In addition to their lower energy inputs during production, such bone chars showed below threshold of the European heavy metal content, in opposite of Cd for calcined sample. Although adding activation steps with N_2 are costlier than pyrolysis in a sealed chamber, the first treatment resulted in the most soluble material at 500 °C, but with lower total P content. The lower the total P content, the higher the transportation costs.

Nonetheless, a less P-concentrated bone char requires higher fertilizer volumes, allowing a better distribution in the field and increasing its reactivity and P interception by plant roots.

Water and neutral ammonium citrate extractable P were negligible compared to citric acid because our bone chars were mostly composed of hydroxyapatite (Ca:P = 1.67), which has lower solubility in optimal pH values for cultivation (~5.5-7) than calcium phosphates with lower Ca:P ratio (e.g. mono and dicalcium phosphates) (LINDSAY, 1979). Since bone chars have a basic pH and their solubilization would result in soil alkalinization, bone chars would be more effective at releasing P to plants in acidic soils than calcareous soils. The greater solubility of HAP in acidic conditions can be verified by the ~130 and ~20-fold higher extractable P by 2% citric acid than water and neutral ammonium citrate, respectively. In addition, we argue that bone char reaction is improved in clayey soils once there is an increased buffer capacity as a result of hydrolysis of Al from soil mineral dissolution. Decomposition of organic matter, (which is higher in these soils) would also participate at dissolving HAP from bone chars (HAVLIN et al., 2005; NANZER et al., 2014). On the other hand, H^+ extrusion by roots and microbial activity, allied to the nitrification of fertilizers or mineralization of NH_4^+, both contributing to soil acidification, are expected to have a higher participation in bone char dissolution in sandy soils, once their lower amount of Al minerals and organic matter results in diminished H^+ release to soil solution.

Bone char pH increases with temperature once accumulation of basic cations (e.g. Mg, Ca, Na, K) in the ash fraction occurs as organic compounds are volatilized with temperature increasing. These cations are accumulated mainly as oxides, carbonates and salts (VASSILEV et al., 2013). In the case of calcination and steam activated (800 °C) treatments, they caused greater organic losses and also presented higher pH compared to the other treatments due to the increased alkaline metals accumulation (Tables 1.4 and 1.5). The high pH of bone chars increases soil pH in surrounding bone char particles areas, inhibiting HAP dissolution and further P release. For this reason, soil buffer capacity drives bone char dissolution in soils, as cited above.

The dissolution rate of bone chars in soils might not provide enough P to completely attend plant requirements once just a small fraction of bone char is water-soluble. Because bone char P release is mediated by soil acidity, higher doses of application; adding composting/fermentation steps to naturally solubilize P from bone char; or fertilization using a combination of bone char with readily available P sources could be used to overcome such limitation. Bone char contains other nutrients such as Mg, K, and Zn and has the advantage of exhibiting low heavy metal amount (mainly Cd) compared to phosphate rock-based fertilizers.

1.5. Conclusion

Pyrolysis of swine bones has both environmental and agricultural benefits, including providing a source of plant-available P by recycling a waste material from the meat industry and reducing disease sources in the bones. Given that the world produces currently around 800 million swine heads yearly, with an average of 15 kg of bones each (in an animal with 100 kg), bone char has a potential to replace six percent of the total P used in agriculture each year (taking year 2000 as basis for consumed P in agriculture) considering a bone char (~18% P) yield around 40% (IRGANG, 1986; MACDONALD et al., 2011). Bone char use could be directed not only for agricultural purposes, but also in restoration of degraded and metal-contaminated soils because of its low metal content and capacity to immobilize metals as Cd while providing P to plants (SIEBERS; KRUSE; LEINWEBER, 2013; SIEBERS; GODLINSKI; LEINWEBER, 2014). Recycling a waste material by creating a bone-based fertilizer would increase P rock mines lifespan and alleviate environmental impacts resulted from mining, manufacturing and cross continent transportation of P rock-based fertilizers.

References

AOAC International. 1999. Official methods of analysis. 16th ed. Vol. I. AOAC Int., Arlington, VA.

BERTOLINI , J.; GOSS, N.; CURLING, J. **Production of plasma proteins for therapeutic use.** edited by Joseph, Neil Goss, and John Curling. JohnWiley & Sons, Inc., Hoboken, New Jersey, 2013, 496 p.

BOURDELLE, F.; BENZERARA, K.; BEYSSAC, O.; COSMIDIS, J.; NEUVILLE, D. R.; BROWN, G. E.; PAINEAU, E. Quantification of the ferric/ferrous iron ratio in silicates by scanning transmission X-ray microscopy at the Fe L2,3 edges. **Contributions to Mineralogy and Petrology**, v. 166, n. 2, p. 423–434, 2013.

BROWN, P.; RAU, E. H.; LEMIEUX, P.; JOHNSON, B. K.; BACOTE, A. E.; GAJDUSEK, D. C. Infectivity studies of both ash and air emissions from simulated incineration of scrapie-contaminated tissues. **Environmental Science and Technology**, v. 38, n. 22, p. 6155–6160, 2004.

CARVALHO, A. M. G.; ARAÚJO, D. H. C.; CANOVA, H. F.; RODELLA, C. B.; BARRETT, D. H.; CUFFINI, S. L.; COSTA, R. N.; NUNES, R. S. X-ray powder diffraction at the XRD1 beamline at~LNLS. **Journal of Synchrotron Radiation**, v. 23, n. 6, p. 1501–1506, 2016.

CEZAR, J. C.; FONSECA, P. T.; RODRIGUES, G. L. M. P.; DE CASTRO, A. R. B.; NEUENSCHWANDER, R. T.; RODRIGUES, F.; MEYER, B. C.; RIBEIRO, L. F. S.;

MOREIRA, A. F. A. G.; PITON, J. R.; RAULIK, M. A.; DONADIO, M. P.; SERAPHIM, R. M.; BARBOSA, M. A.; DE SIERVO, A.; LANDERS, R.; DE BRITO, A. N. The U11 PGM beam line at the Brazilian National Synchrotron Light Laboratory. **Journal of Physics: Conference Series**, v. 425, n. PART 7, 2013.

CORDELL, D. Global phosphorus scarcity: A food secure future? **Journal of Nutrition & Intermediary Metabolism**, v. 8, n. 2017, p. 61–62, 2017.

COSMIDIS, J.; BENZERARA, K.; NASSIF, N.; TYLISZCZAK, T.; BOURDELLE, F. Characterization of Ca-phosphate biological materials by scanning transmission X-ray microscopy (STXM) at the Ca L2,3-, P L2,3- And C K-edges. **Acta Biomaterialia**, v. 12, n. 1, p. 260–269, 2015.

CROSS, A.; SOHI, S. P. The priming potential of biochar products in relation to labile carbon contents and soil organic matter status. **Soil Biology and Biochemistry**, v. 43, n. 10, p. 2127–2134, 2011.

ENDERS, A.; LEHMANN, J. Comparison of Wet-Digestion and Dry-Ashing Methods for Total Elemental Analysis of Biochar. **Communications in Soil Science and Plant Analysis**, v. 43, n. 7, p. 1042–1052, 2012.

EUROPEAN COUNCIL. Proposal for a regulation of the European Parliament and of the Council laying down rules on the making available on the market of CE marked fertilising products and amending Regulations (EC) No 1069/2009 and (EC) No 1107/2009. Brussels, 2016.

EU FOOD SAFETY. 2007. Questions and Answers on BSE. Disponível em: < https://ec.europa.eu/food/sites/food/files/safety/docs/biosafety_food-borne-disease_tse_qanda-2007_en.pdf>The Independent. 2000. Parliament: BSE Cost. April 8.

FIGUEIREDO, M.; FERNANDO, A.; MARTINS, G.; FREITAS, J.; JUDAS, F.; FIGUEIREDO, H. Effect of the calcination temperature on the composition and microstructure of hydroxyapatite derived from human and animal bone. **Ceramics International**, v. 36, n. 8, p. 2383–2393, 2010.

HABERKO, K.; BUĆKO, M. M.; BRZEZIŃSKA-MIECZNIK, J.; HABERKO, M.; MOZGAWA, W.; PANZ, T.; PYDA, A.; ZAREBSKI, J. Natural hydroxyapatite - Its behaviour during heat treatment. **Journal of the European Ceramic Society**, v. 26, n. 4–5, p. 537–542, 2006.

HAVLIN, J. L.; BEATON, J.D., TISDALE, S.L.; NELSON, W.L. **Soil Fertility and Fertilizers**. An Introduction to Nutrient Management. Pearson Education, Inc., Upper Saddle River, New Jersey. 2005.

IOANNIDOU, O.; ZABANIOTOU, A. Agricultural residues as precursors for activated carbon production-A review. **Renewable and Sustainable Energy Reviews**, v. 11, n. 9, p. 1966–2005, 2007.

IRGANG, R. Peso ótimo de abate de suínos. v. 21, n. 12, p. 1337–1345, 1986.

ITO, A.; MAEKAWA, K.; TSUTSUMI, S.; IKAZAKI, F.; TATEISHI, T. Solubility product of OH-carbonated hydroxyapatite. **Journal of Biomedical Materials Research**, v. 36, n. 4, p. 522–528, 1997.

JOINT COMMITTEE ON POWDER DIFFRACTION STANDARDS (JCPDS). S**elected powder diffraction data for minerals**. JCPDS, Philadelphia, PA. 1974.

JOSEPH, S. D.; CAMPS-ARBESTAIN, M.; LIN, Y.; MUNROE, P.; CHIAA, C. H.; HOOK, J.; ZWIETEN, L. van; KIMBER, S.; COWIE, A.; SINGH, B. P.; LEHMANN, J.; FOIDL, N.; SMERNIK, R. J.; AMONETTE, J. E. CSIRO PUBLISHING - Soil Research An investigation into the reactions of biochar in soil CSIRO PUBLISHING - Soil Research. **Australian Journal of Soil Research**, v. 48, n. iv, p. 501–515, 2010.

KHOO, W.; NOR, F. M.; ARDHYANANTA, H.; KURNIAWAN, D. Preparation of Natural Hydroxyapatite from Bovine Femur Bones Using Calcination at Various Temperatures. **Procedia Manufacturing**, v. 2, n. February, p. 196–201, 2015.

LANDI, E.; CELOTTI, G.; LOGROSCINO, G.; TAMPIERI, A. Carbonated hydroxyapatite as bone substitute. **Journal of the European Ceramic Society**, v. 23, n. 15, p. 2931–2937, 2003.

LINDSAY, W. L. John Wiley and Sons Ltd., Chichester, Sussex, UK 1979. 449 p.

LOMBARDI, M.; PALMERO, P.; HABERKO, K.; PYDA, W.; MONTANARO, L. Processing of a natural hydroxyapatite powder: From powder optimization to porous bodies development. **Journal of the European Ceramic Society**, v. 31, n. 14, p. 2513–2518, 2011.

MACDONALD, G. K.; BENNETT, E. M.; POTTER, P. A.; RAMANKUTTY, N. Agronomic phosphorus imbalances across the world's croplands. **Proceedings of the National Academy of Sciences**, v. 108, n. 7, p. 3086–3091, 2011.

MAHISARAKUL, J.; SIRIPAIBOOL, C.; CLAIMON, J.; PAKKONG, P. field assessment of the relative agronomic effectiveness of phosphate rock materials in a soybean — maize crop rotation using 32p isotope techniques. In: **Assessment of soil phosphorus status and management of phosphatic fertilisers to optimize crop production.** ISSN 1011–4289, Vienna, 2002.

MANCEAU, A.; MARCUS, M. A.; GRANGEON, S. Determination of Mn valence states in mixed-valent manganates by XANES spectroscopy. **American Mineralogist**, v. 97, n. 5–6, p. 816–827, 2012.

MAYER, I.; FEATHERSTONE, J. D. B. Dissolution studies of Zn-containing carbonated hydroxyapatites. **Journal of Crystal Growth**, v. 219, n. 1–2, p. 98–101, 2000.

NANZER, S.; OBERSON, A.; BERGER, L.; BERSET, E.; HERMANN, L.; FROSSARD, E. The plant availability of phosphorus from thermo-chemically treated sewage sludge ashes as studied by 33P labeling techniques. **Plant and Soil**, v. 377, n. 1–2, p. 439–456, 2014.

OXMANN, J. F. Technical note: An X-ray absorption method for the identification of calcium phosphate species using peak-height ratios. **Biogeosciences**, v. 11, n. 8, p. 2169–2183, 2014.

PATEL, S.; WEI, S.; HAN, J.; GAO, W. Transmission electron microscopy analysis of hydroxyapatite nanocrystals from cattle bones. **Materials Characterization**, v. 109, p. 73–78, 2015.

RAJENDRAN, J.; GIALANELLA, S.; ASWATH, P. B. XANES analysis of dried and calcined bones. **Materials Science and Engineering C**, v. 33, n. 7, p. 3968–3979, 2013.

RAJKOVICH, S.; ENDERS, A.; HANLEY, K.; HYLAND, C.; ZIMMERMAN, A. R.; LEHMANN, J. Corn growth and nitrogen nutrition after additions of biochars with varying properties to a temperate soil. **Biology and Fertility of Soils**, v. 48, n. 3, p. 271–284, 2012.

RAVEL, B.; NEWVILLE, M. ATHENA, ARTEMIS, HEPHAESTUS: data analysis for X-ray absorption spectroscopy using IFEFFIT, **Journal of Synchrotron Radiation**, v. 12, p. 537–541, 2005.

REY, C.; COMBES, C.; DROUET, C.; GLIMCHER, M. J. Bone mineral: Update on chemical composition and structure. **Osteoporosis International**, v. 20, n. 6, p. 1013–1021, 2009.

SCHIMMELPFENNIG, S.; GLASER, B. One Step Forward toward Characterization: Some Important Material Properties to Distinguish Biochars. **Journal of Environment Quality**, v. 41, n. 4, p. 1001, 2012.

SMITH, J. J. The taking of the Sahara: the role of natural resources in the continuing occupation of Western Sahara. **Global Change, Peace and Security**, v. 27, n. 3, p. 263–284, 2015.

SOBCZAK-KUPIEC, A.; WZOREK, Z. The influence of calcination parameters on free calcium oxide content in natural hydroxyapatite. **Ceramics International**, v. 38, n. 1, p. 641–647, 2012.

TAYLOR, D. M.; FRASER, H.; MCCONNELL, I.; BROWN, D. A.; BROWN, K. L.; LAMZA, K. A.; SMITH, G. R. A. Decontamination studies with the agents of bovine spongiform encephalopathy and scrapie. **Archives of Virology**, v. 139, n. 3–4, p. 313–326, 1994.

TRUONG; B.J.; F. ZAPATA. Standard characterization of phosphate rock samples from the FAO/IAEA phosphate project. In: **Assessment of soil phosphorus status and management of phosphatic fertilisers to optimize crop production**. ISSN 1011–4289, Vienna, 2002.

VAN VUUREN, D. P.; BOUWMAN, A. F.; BEUSEN, A. H. W. Phosphorus demand for the 1970-2100 period: A scenario analysis of resource depletion. **Global Environmental Change**, v. 20, n. 3, p. 428–439, 2010.

VASSILEV, S. V; BAXTER, D.; ANDERSEN, L. K.; VASSILEVA, C. G. An overview of the composition and application of biomass ash . Part 1 . Phase – mineral and chemical composition and classification. **Fuel**, v. 105, p. 40–76, 2013.

Supporting information

Table S1.1 Full width at half maximum (FWHM) of 002 peak from hydroxyapatites present in bone chars produced under different temperatures and atmosphere compositions and standard pure hydroxyapatites.

Bone treatment	FWHM (° 2θ)
Dried Bone	0.232
BC 400 °C	0.187
BC 550 °C	0.185
BC 550 °C (N_2)	0.221
BC 800 °C	0.193
BC 800 °C (N_2)	0.204
BC 800 °C (WV)	0.082
CA 800 °C	0.048
Hydroxyapatites	
Reagent grade	0.115
Reagent grade, nano-sized[†]	0.082
Synthesized at 90 °C	0.036

BC: Bone char; N_2: nitrogen activation; WV: steam activation; CA: calcination

Table S1.2 Energy step sizes used to acquire P and Ca K-edge XANES spectra of bone char and standard samples.

Element	From	To	0.2 ev	1 eV	3 eV
	eV				
P	2120	2145		**x**	
	2145.2	2180	**x**		
	2181	2220		**x**	
	2223	2300			**x**
Ca	4000	4030		**x**	
	4030.2	4070	**x**		
	7071	4100		**x**	
	4103	4200			**x**

Table S1.3 List of standards used in phosphorus (P) and calcium (Ca) K and L-edge XANES spectra comparison.

	Chemical Formula	P		Ca	
		K-edge	L-edge	K-edge	L-edge
Phytic Acid	$C_6H_{18}O_{24}P_6$		x		x
Amorphous Calcium Phosphate	$Ca_2O_7P_2.H_2O$	x		x	
Monocalcium Phosphate	$Ca(H_2PO_4)_2$	x	x		x
Dicalcium Phosphate	$CaHPO_4$	x	x		x
Brushite	$CaHPO_4.2H_2O$		x		x
β-tricalcium phosphate	$Ca_3(PO_4)_2$	x	x	x	x
Octacalcium Phosphate	$Ca_8H_2(PO_4)_6.5H_2O$		x		x
Reagent grade HAP (LO)	$Ca_5(PO_4)_3(OH)$	x	x	x	x
Nano-sized reagent grade HAP	$Ca_5(PO_4)_3(OH)$		x		x
Lab. Synthesized HAP (HO)	$Ca_5(PO_4)_3(OH)$		x		x
Calcite	$CaCO_3$			x	x
Calcium oxide	CaO				x
Ca-cellulose	$Ca\text{-}(C_6H_{10}O_5)_n$			x	
Calcium Chlorine	$CaCl_2$			x	
Calcium sulfate	$CaSO_4$			x	

LO: low ordered; HI: highly ordered

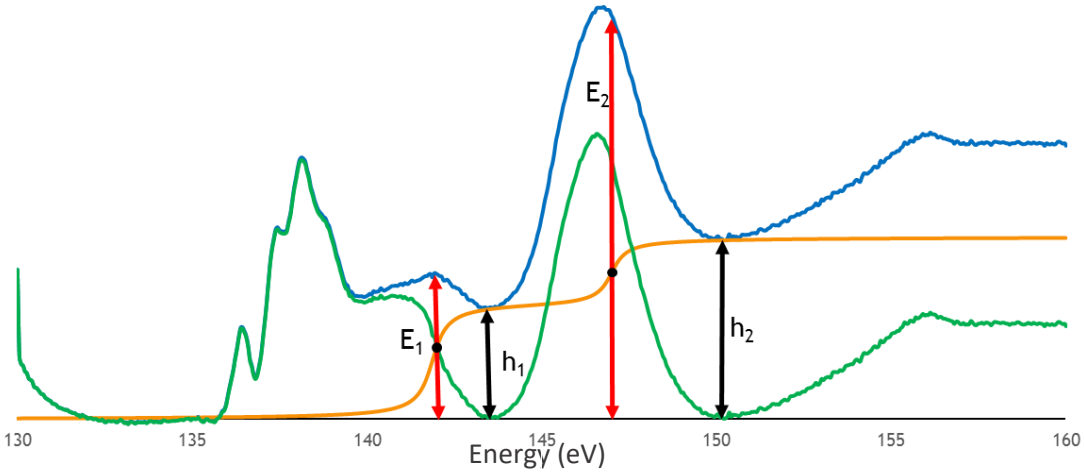

Figure S1.1 Example of baseline correction applied in XANES spectra of P $L_{2,3}$-edge (the same was performed for Ca $L_{2,3}$-edge) by subtracting a double arctan function after its adjustment through function (1). E1 was set to the border of a shoulder around 142 eV, and E2 was fixed to 147.5 eV for the peak with a maximum around 147 eV for P, whereas in Ca spectra E1 and E2 were set to 347.73 and 353 eV, respectively. The parameters h_1 and h_2 were set as minimum after E_1 and E_2. Blue line: raw spectrum; orange line: adjusted arctan function; green line: baseline corrected spectrum (subtracted by arctan function). Note that E_1 and E_2 correspond to the energy of the arctan function intersection point.

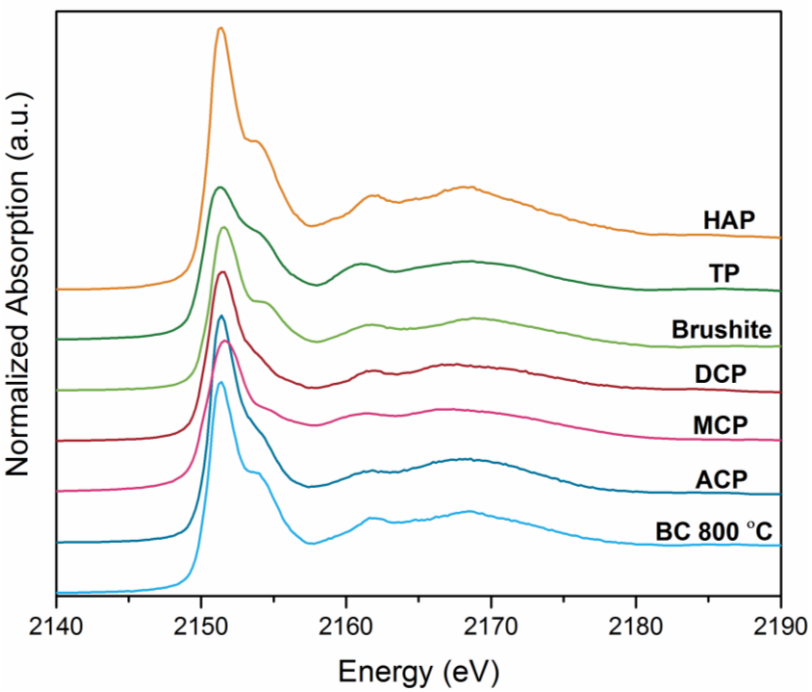

Figure S1.2 XANES P K-edge spectra of reagent grade P compounds and a sample of bone char (BC) for comparison purposes. HAP: hydroxyapatite; TP: β-tricalcium phosphate; DCP: dicalcium phosphate; MCP: monocalcium phosphate; ACP: amorphous calcium phosphate.

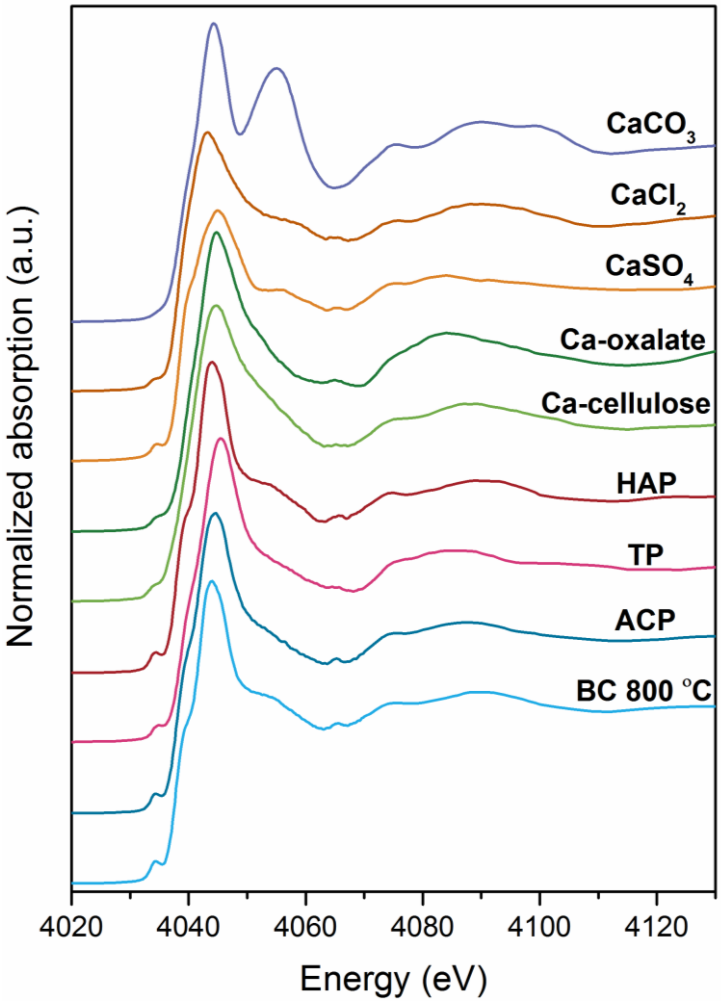

Figure S1.3 XANES Ca K-edge spectra of reagent grade calcium compounds and a sample of bone char (BC) for comparison purposes. HAP: hydroxyapatite; TP: β-tricalcium phosphate; ACP: amorphous calcium phosphate.

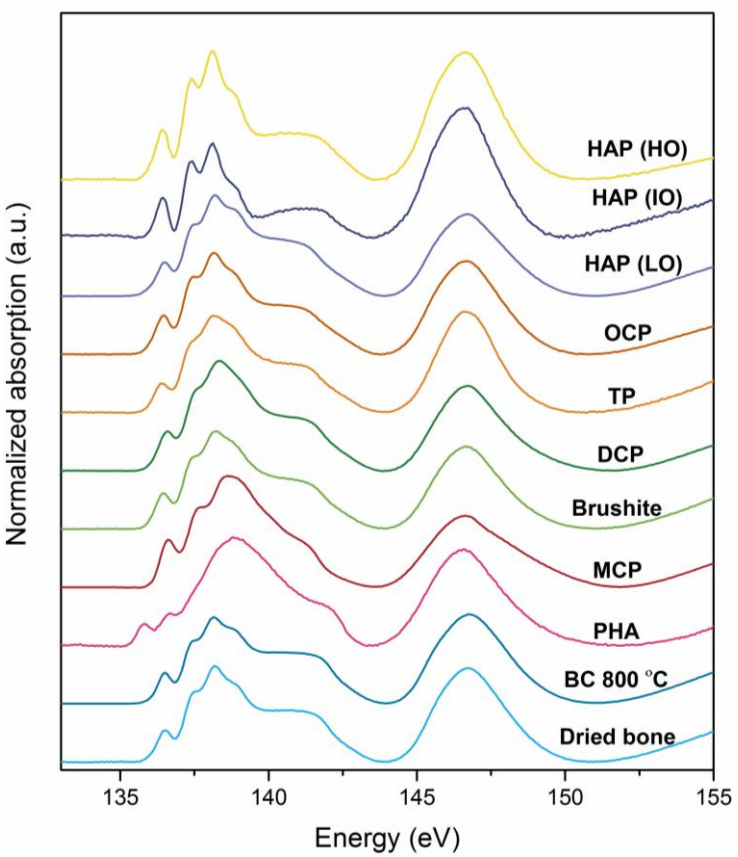

Figure S1.4 XANES P L-edge spectra of reagent grade phosphate compounds and dried bone and a sample of bone char (BC) for comparison purposes. HAP: hydroxyapatite; TP: β-tricalcium phosphate; DCP: dicalcium phosphate; MCP: monocalcium phosphate; ACP: amorphous calcium phosphate.

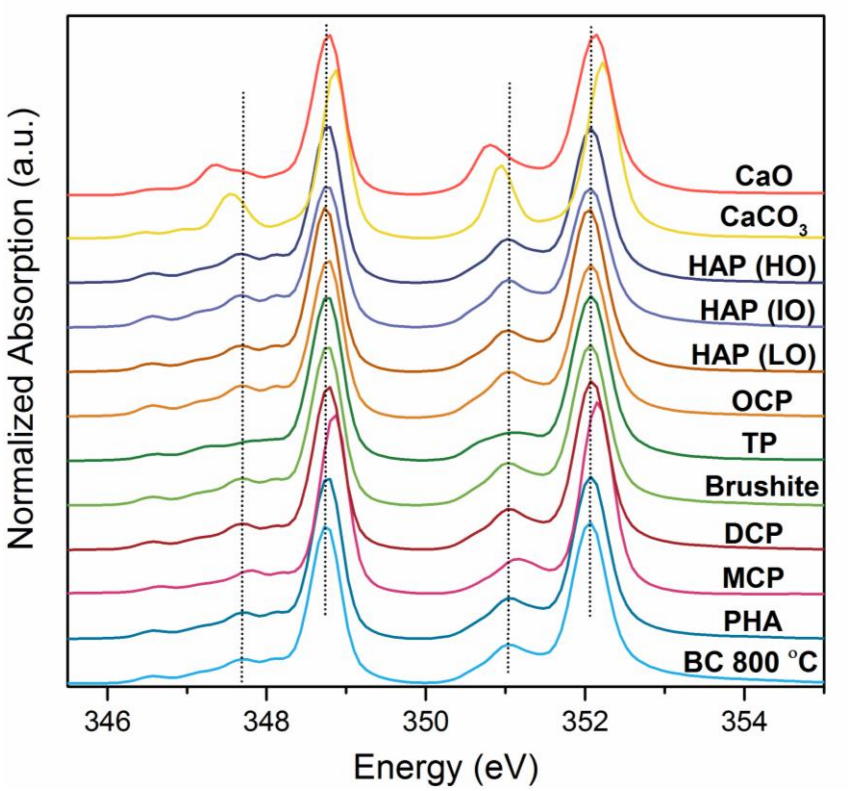

Figure S1.5 XANES Ca L-edge spectra of reagent grade calcium compounds and a sample of bone char (BC) for comparison purposes. HAP: hydroxyapatite; HO: high ordering; IO: intermediary ordering; LO: low ordering; OCP: octacalcium phosphate; TP: β-tricalcium phosphate; DCP: dicalcium phosphate; MCP: monocalcium phosphate; ACP: amorphous calcium phosphate. PHA: phytic acid. Dotted vertical lines support peak position visualization.

2. PYROLYSIS AS ALTERNATIVE TO CALCINATION FOR BONE-BASED FERTILIZER GENERATION

Abstract

Pyrolysis can be an efficient technique to treat bones and generate an efficient phosphate fertilizer. Our objective was to test a set of bone chars regarding phosphorus release kinetics and verify plant P absorption from these bone chars in a pot experiment, using calcined bones and phosphate rock-based fertilizers as standard treatments. Bone chars obtained at 400, 550 and 800 °C in sealed chamber, 800 °C under steam activation and calcination at 800 °C were submitted to a stirred-chamber experiment aiming to access the $t_{1/2}$ (time necessary for bone char releasing half of total P released during 2h of 2% formic acid flux). In a pot experiment, the same bone chars were added in labelled sandy and clayey soils in order to measure plant growth, total P uptake per pot, P absorbed uniquely from the fertilizers and the percentage of fertilizer used by rice plants. Bone char 400 °C showed in both soils an efficiency comparable to phosphate rock. Previous characterization of the tested materials suggests that the main factors involved in the P release from bone char in stirred-flow chamber P release and greenhouse experiments was the crystallinity of bone char allied to physical properties such as porosity and surface area. Although 550 and 800 °C bone chars produced in sealed chamber released the P faster, they were not as efficient as 400 °C bone char at providing P to plants. Although calcination is widely employed as bone treatment, the capability of this material to provide P to plants is much lower than bone chars produced in sealed chamber. Therefore, pyrolysis is an alternative technique to treat bones instead of using calcination.

Keywords: Charred bones; Calcined bones; Labelled phosphorus

2.1. Introduction

Phosphorus is macronutrient for all living organisms. In the case of plants, suitable P contents in the soil for feasible crop yields require intense use of fertilizers, mainly in high-P fixing soils where the adsorptive potential of aluminum (Al) and iron (Fe) oxides reduce their efficiency (SPARKS, 2007).

Once phosphate rocks are being depleted and their sources are non-renewable, it is necessary to discover new phosphate sources to recycle, at least in part, the existing common fertilizers (CORDELL, 2017). In Europe for example, almost all mineral phosphate fertilizers utilized in agriculture are imported, similarly to the occurred in India. In Brazil, around 70% of the P fertilizers are imported (NATIONS, 2014). Researchers pointed out that in a future with scarce P sources, Brazilian agriculture, for example, might become not as competitive as today due to the increased application rates of P fertilizers compared to non-tropical countries (ROY et al., 2016). The same is expected for the other countries located in other tropical regions with intense agriculture.

Bones are a rich-P source and could recycle part of the P utilized as fertilizer in agriculture. Some studies point out that bones can be as efficient as water-soluble fertilizers, nonetheless the material characteristics that act controlling its efficiency are mainly only attributed to mineral disorder of hydroxyapatite nanocrystals, which are the principal minerals phase of bones (ZWETSLOOT; LEHMANN; SOLOMON, 2015). Nevertheless, a treatment prior further destination is demanded in order to produce a suitable fertilizer. Although calcination of bones is a common bone treatment, it could result in decreased efficiency of the resultant material as a fertilizer due to changes in the mineral structure of hydroxyapatite. Pyrolysis is an alternative thermal treatment that could be used to generate an effective P fertilizer from bones. The effectiveness of bone chars is not well documented; however different pyrolysis settings could generate bone-based fertilizers with contrasting characteristics (showed in chapter 1) and efficiencies.

Besides chemical and physical characteristics, solubility of bone chars in soils is driven by the same factors as those of phosphate rock (P rock), such as soil buffer capacity. This implies that bone char efficacy as fertilizer would be augmented if applied in acidic clayey soils that have higher buffer capacity than sandy or calcareous soils (WARREN; ROBINSON; SOMEUS, 2009). Our objective was to evaluate the efficacy of contrasting bone chars at providing P to plants compared to calcined bones and P rock-based fertilizers. A P release

kinetic study and a pot experiment using two soils with different sorption capacities were utilized to reveal bone char and other P fertilizers effectiveness.

2.2. Material and Methods

Bone chars cited in the chapter one were here further investigated regarding P release in 2% formic acid in stirred-flow mode and in a pot experiment with ^{32}P labelled soils (sandy and clayey) with different buffering capacities. In order to understand the influence of bone char quality in plant P absorption, bone chars were selected according to contrasting physical and chemical attributes. Therefore, bone chars (<0.250 mm) produced from swine bones at 400, 550 and 800 °C in sealed chamber; steam activation and calcination (calcined bones), both at 800 °C, were utilized. Calcined bones were utilized as control treatment.

2.2.1. Bone char P release kinetics

To test bone char P releasing behavior, 50 mg of each sample was placed into a micro stirred-flow chamber, which was mounted between a tubing pump and a fraction collector. Two percent formic acid was utilized to mimic plant extraction instead of 2% citric acid since it had a higher correlation with plant uptake in tests involving charred vegetal biomass (biochar) with high ash content (WANG, 2012).

Extract fractions of two milliliters were automatically collected at every three minutes for two hours by using a chromatography fraction collector. Phosphorus content in the extracts was accessed by spectrophotometry after testing the possible interference of formate in color development, which was proven to be indifferent (MURPHY; RILEY, 1962).

Bone char dissolution data was adjusted through the use of CurveExpert® to a logistic function ("S" shape/sigmoidal curve) where coefficients a, b and c were estimated according to reaction time *versus* the relative P release (accumulated/total release), as follows:

$$\boldsymbol{q = \frac{a}{1 + be^{-ct}}} \qquad (1)$$

q: relative P release
a: the curve's maximum value
b: the y-intercept
c: the growth rate
e: the natural logarithm base
t: time (min)

The validity of *a*, *b* and *c* estimative was accessed through calculating a 95% confidence interval in SAS® and checking interval zero presence. When zero was not in the interval, we assumed that the coefficient was significantly different from zero at 5% significance level. Thereafter, experimental and estimated *q* values were adjusted to a linear function and adjusted-R^2 was calculated to indicate the goodness of the estimative.

The reaction time of bone char and formic acid 2% necessary to provoke a release equal to half of total released P ($t_{1/2}$) was accessed through equation (1) by equaling *q* to 0.5.

2.2.2. Plant ^{32}P uptake from fertilizers

To test bone char performance as P fertilizer, bone chars cited above were compared to phosphate rock (bayovar) and super triple phosphate (STP) as standard P fertilizers. Bayovar is a sedimentary phosphate rock (13.1% P) from Peru, destined for direct application in soils as a fine powder. P rock was utilized as a slow-release source that depends on soil buffer capacity to dissolve, similarly to bone chars. Super triple phosphate (19.9% P) is a fully acidulated P fertilizer obtained through adding phosphoric acid to low reactive P rock (igneous origin) in order to solubilize P minerals, turning the product soluble in water. Such fertilizer quickly provides phosphorus to plants after field application.

A sandy and clayey soils with different P adsorption capacities classified as Ferralsol (WRB, 2014) were collected in Brazil (Piracicaba, Sao Paulo). They were employed to test bone char effectiveness in soil conditions. The clay fraction of both soils was composed by kaolinite, hematite, gibbsite, goethite and quartz (AVILA, 2016). Clayey Ferralsol contained 290, 163 and 547 g kg^{-1} of sand, silt and clay, respectively, and could adsorb a maximum of 1495 mg kg^{-1} of P (given by Langmuir isotherm), while sandy soil showed respectively 760, 21 and 219 g kg^{-1} of sand, silt and clay, and a P maximum adsorption capacity of 660 mg kg^{-1}. Organic matter content was 24 and 38 mg dm^{-3} in sandy and clayey soil, respectively. Further soil characterization is shown in Table 2.1. Soils (<4mm) were limed to attain base saturation around 50%, according to regional bulletin of soil fertility (RAIJ, 1997), and 50 mg kg^{-1} nitrogen [$(NH_4)_2SO_4$], 40 mg kg^{-1} potassium (K_2SO_4) and 1 mg kg^{-1} of boron (H_3BO_3), copper ($CuCl_2$. $2H_2O$) and zinc ($ZnCl_2$) were added to soil as solution.

Table 2.1 Characteristics of the soils used in the pot experiment, after liming

Soil	P	S	B	Cu	Fe	Mn	Zn	K	Ca	Mg	Al	H+Al	SB	CEC	pH	V
	mg dm^{-3}							$mmol_c$ dm^{-3}								%
Sandy	10	15	0.3	0.9	86	46.8	2.1	0.4	23	9	<1	18	32.4	50.4	4.8	64
Clayey	10	11	0.2	1.2	46	29.1	2.2	1.1	27	12	<1	28	40.1	68.1	4.8	59

S: SB: sum of bases; CEC: cation exchange capacity; V: base saturation; m: aluminum saturation in effective CEC. Extraction methods: P, Ca, Mg, K: resin; B: hot water; Fe, Cu, Mn, Zn: DTPA; Al: KCl 1 M; S: calcium phosphate 0.01 M; organic matter (OM): oxidation by dichromate in acid media. Potential acidity (H+Al) determined by pH in SMP buffer

Spiking 4.7 MBq of ^{32}P radionuclide (β particle emitter) in 30 mL of sand was performed to label soil P in all its fractions (e.g. plant available, adsorbed, precipitated) by means of isotopic equilibrium. Sand was allowed to dry at room temperature and then thoroughly mixed with 2 kg of soil (<4 mm) that had been previously placed into reinforced plastic bags. After, plastic bags containing soils were placed in plastic pots, moisturized to attain 70% of maximum water holding capacity (MWHC), sealed (to avoid water evaporation) and incubated for 15 days to allow isotope equilibrium. Once isotopic equilibrium is approached, plant will proportionally uptake ^{31}P and ^{32}P from soil different fractions (VOSE, 1980). Pots were unsealed after 15 days and allowed to dry. Finally, 30 mg kg^{-1} P from each fertilizer was applied (P rock and bone chars as powder and STP as granules).

Seeds of an upland rice, cultivar Sinuelo CL (Brazilian cultivar) were sown at two centimeters depth. The selected cultivar was responsive to P addition and efficient at absorbing P (MARCANTE, 2015). Soil was kept at 70% of MWHC and additional 50 mg kg^{-1} N and 40 mg kg^{-1} K were applied to pots when rice plants were at the tillering stage. Plant shoot was harvested at 50 days after seed germination, dried (65 °C), weighed, ground, digested (HNO_3:$HClO_4$, 5:1), diluted to 20 mL and analyzed in terms of ^{31}P (stable) content by spectrophotometry using the vanadate-yellow color method (JACKSON, 1973). The disintegration of ^{32}P atoms from plant-digested solution was counted through Cerenkov effect in water media (VOSE, 1980). Accumulated P in shoot [dried shoot biomass (g/pot) × P content (g kg^{-1}) = P accumulated (g/pot)] and P in shoot absorbed exclusively from bonechar or fertilizer were calculated, as follows:

Specific activity of ^{32}P in plant shoot tissue:

SAc: specific activity (Bq mg^{-1})

$$SAc = \frac{^{32}P}{^{31}P} \quad (2)$$

^{32}P: ^{32}P radionuclide activity in the plant (Bq)

^{31}P: plant P content (mg g^{-1})

Phosphorus derived from fertilizer (Pdf):

$$Pdf = 1 - \left[\frac{SAc_{(Fertilizer+Soil)}}{SAc_{(Soil)}}\right] \quad (3)$$

Pdf: P fraction in plant shoot derived from fertilizer (Pdf)

$SAc_{(Fertilizer + Soil)}$: P specific activity in the plant that was absorbed from fertilizer + soil

$SAc_{(Soil)}$: P specific activity of plants cultivated in control treatment (no P addition)

P uptake by plant exclusively from fertilizer:

$$P_{uf} = Pdf_{fertilizer} \times P_{acum\ (fertilizer+soil)} \quad (4)$$

P_{uf}: P uptake from fertilizer (µg/pot)

$P_{acum\ (Fertilizer + Soil)}$: total P content in plant shoot (µg/pot)

Obs. P_{uf} was divided by 1000 to transform from µg to mg/pot.

Collected data was submitted to analysis of variance by using SAS®. When necessary, data was transformed to attain ANOVA assumptions. Treatment means were compared through Tukey's test ($p \leq 0.05$).

2.3. Results and Discussion

2.3.1. Bone char P release kinetics

Because samples showed no further P release after one hour of bone char dissolution in 2% formic acid, data modeling comprehended only the first hour of reaction.

All bone chars and calcined bone sample had a relative P release that was explained by a logistic function/curve (Table 2.1). The $t_{1/2}$ is shown in Table 2.2, which gives information regarding how easy a bone char can be dissolved by acid formic 2% and release P ($t_{1/2}$ is the period of time needed for a bone char release half of the total P released during the experiment). The lower the $t_{1/2}$ value, the faster P can be delivered to "plants", without considering soil media.

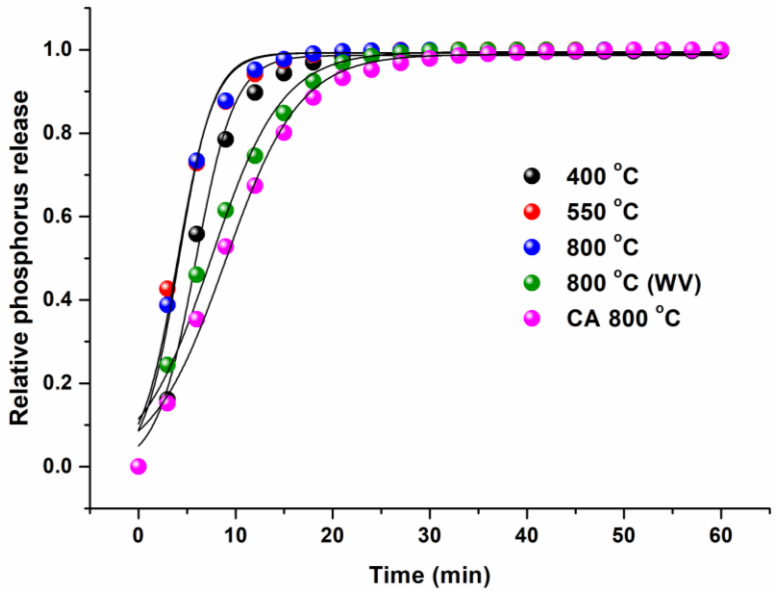

Figure 2.1. Phosphorus releasing temporal evolution by bone chars produced at 400, 550 and 800 °C in sealed chamber, 800 °C steam activated bone char (WV) and calcined bones (CA), submitted to 2% formic acid extraction in stirred-chamber.

Table 2.2 Adjustment results of the logistic function for phosphorus releasing kinetics

Fonte	*a* [1]	*b* [2]	*c* [3]	$t_{1/2}$ [4] (min)	a [6]	b [6]	R^2 [7]
400 °C	0,9865 (0,9737 - 0,9994)	18,7657 (10,4785 - 27,0529)	0,4974 (0,4263 - 0,5685)	6	-0,0287 (-0,0632 - 0,0058)	1,0302 (0,9922 - 1,0681)	0,9938
550 °C	0,9922 (0,9753 - 1,0092)	08,6427 (04,4913 - 12,7942)	0,5354 (0,4279 - 0,6430)	4,1	-0,0459 (-0,1019 - 0,0101)	1,0478 (0,9877 - 1,1078)	0,9852
800 °C	0,9929 (0,9785 - 1,0073)	10,2153 (05,7310 - 14,6996)	0,5595 (0,4629 - 0,6561)	4,2	-0,0407 (-0,0870 - 0,0055)	1,0423 (0,9927 - 1,0919)	0,9898
800 °C (WV)	0,9952 (0,9763 - 1,0142)	07,7023 (05,0380 - 10,3667)	0,2739 (0,2317 - 0,3160)	7,5	-0,0306 (-0,0774 - 0,0162)	1,0328 (0,9802 - 1,0854)	0,9883
800 °C CA	0,9889 (0,9733 - 1,0046)	10,5208 (07,3544 - 13,6872)	0,2626 (0,2311 - 0,2941)	9,1	-0,0258 (-0,0595 - 0,0079)	1,0281 (0,9893 - 1,0668)	0,9936

s(1), (2) e (3) Coeficient estimatives of the function $q = a / (1 + be^{-ct})$; (4) time necessary for half of the P releasing evaluated during the experimental period, min.; (5), (6) e (7) respectives linear, angular and determination coefients of the equation $y = a + bx$, where y and x correspond, respectively, to the P relative releasing measured experimentally and to the phosphorus releasing estimated by logistic function. Values between parenthesis correspond to the confidence interval of the coefficient estimative calculated with 95% of probability.

Bone chars produced at 550 and 800 °C exhibited the fastest P release (~4 min) estimated by the logistic function and given by $t_{1/2}$, while 400 °C showed a value equal to 6 min. Steam activation and calcination provoked crystallite size increase and lower pore volume (results from chapter 1), which could possibly caused the higher $t_{1/2}$ values (7.5 and 9.1 min, respectively) compared to bone chars obtained in sealed chamber. The crystallite size and higher amounts of ACP-like compounds in bone chars produced in sealed chamber seems to drive bone char dissolution pattern. However, the slower dissolution rate of bone char 400 °C could be explained by its decreased surface area and porosity, which were respectively 3 $m^2 g^{-1}$ and 0.01 $cm^3 g^{-1}$, compared to an average of 87.5 $m^2 g^{-1}$ and 0.15 $cm^3 g^{-1}$ for bone chars produced at 550 and 800 °C in sealed chamber. Because 400 °C exhibited a lower porosity and surface area and less crystalline hydroxyapatite, this bone char could reveal a dissolution rate in soils more compatible to plant needs than the other biochars, being not too soluble as 500 and 800 °C sealed chamber bone chars and not too insoluble as calcined bone and steam activated bone char.

2.3.2. Plant ^{32}P uptake from fertilizers

All bone chars showed to be more efficient than calcined bones. In sandy and clayey soils, the fertilizer use for 400 °C bone char produced in sealed chamber was around 3 and 10-fold higher than calcined bones. Total P in shoot per pot, fertilizer absorbed only from fertilizer and fertilizer use trended with pyrolysis temperature for materials obtained in sealed chamber. On the other hand, when steam activation (steam contained reactive water) and calcination in open atmosphere were employed both at 800 °C, the efficiency of the generated bone chars decreased in comparison to 800 °C bone char produced in sealed chamber. The increased crystallinity of calcined bone and steam activated bone char sample diminished the solubility of these materials and their efficiency as fertilizers.

In agreement with the exposed in the section 2.3.1 results, fertilizer use in percentage was highest for bone char 400 °C compared to the other bone fertilizers. This bone char had lower porosity and greater fraction of P-Ca compounds composed by ACP-like structures when compared to the other tested bone-based fertilizers, being the latter characteristic demonstrated in chapter 1 through LCF fitting of XANES Ca K-edge spectra.

It is important to note the advantage of using labelling techniques for the estimative of fertilizer use by plants. Phosphorus uptake, obtained through conventional methods, was equivalent between 400 and 550 °C sealed chamber bone chars. On the other hand, the variables

fertilizer use and P uptake from fertilizer, which were calculated from soil ^{32}P labelling, differentiated 400 and 550 °C bone chars in both soils, indicating the advantage of this methods once the amount of P absorbed from the different sources (soil and fertilizer) are separated.

The faster P release (lower $t_{1/2}$) of 550 and 800 °C bone chars caused lower total P uptake and fertilizer use by plants compared to 400 °C, STP and P-rock, probably due to their rapid fixation in the soil and decreased capacity to replace the fixed P to soil solution (Figures 2.3 and 2.4).

Bone char obtained at 400 °C was similar to STP in the clayey soil. On the other hand, in the sandy soil where plant dry matter and P use from bone char decreased obeying the order:

STP > P rock = 400 °C > 550 °C = 800 °C > steam activated bone char > calcined bone

The trend in dry matter production was not as contrasting as P uptake and varied from ~8 to 13 g per pot, differently of clayey soil with values ranging from ~3 to 13 g/pot. The lower capacity of sandy soil to provide H^+ to solution resulted in lesser dissolution of bone chars and P rock (HAVLIN et al., 2005).

Fertilizer use was around 23% for STP in sandy soil and around 18 for clayey soil. For bone char 400 °C, the most efficient, P used from fertilizer was 15% in average. These results show the challenges linked to P fertilization and food secure in a near future. Most applied P is not used by plants in a first cropping season; however, fertilizers with low solubility such as bone char and P-rock, which demand H^+ (part released by plant roots) to dissolve, could be further used in next cultivation seasons. The P sources are non-renewable and low gains in terms of fertilizer efficiency and use by plants might be significant for decelerating P mines depletion.

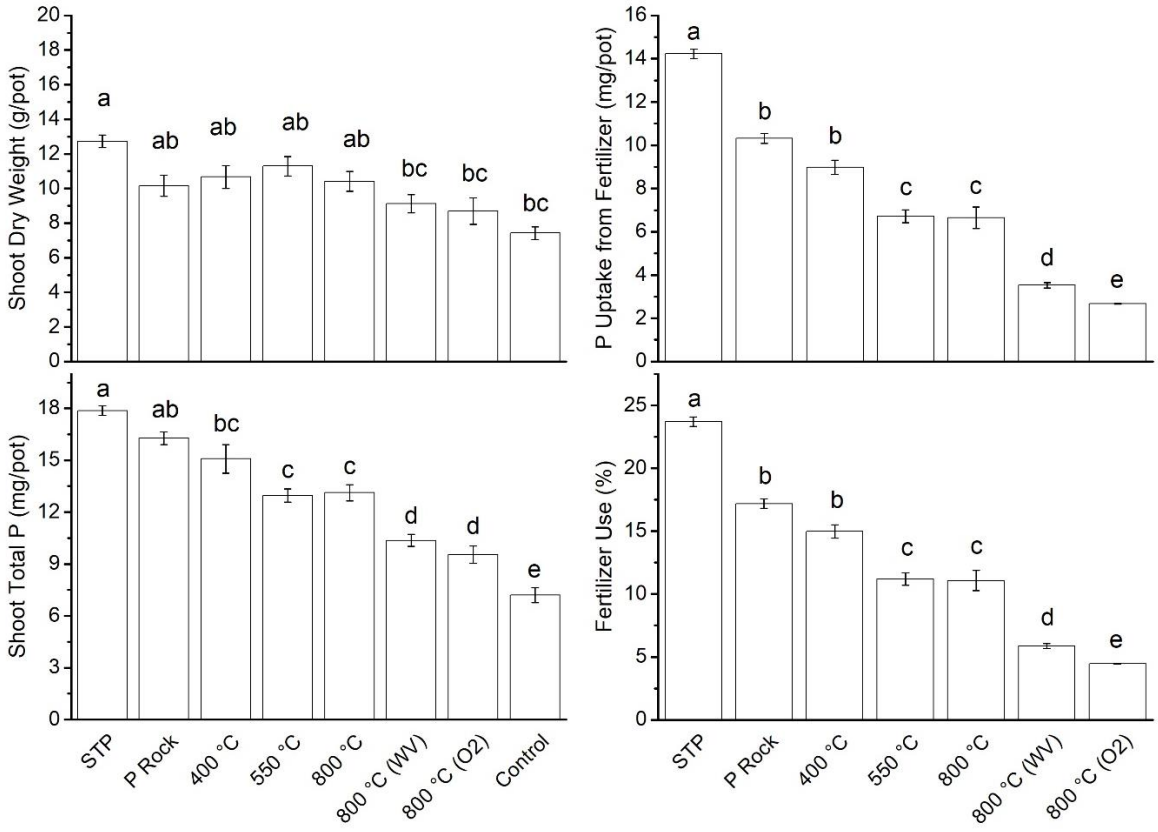

Figure 2.3 Shoot dry matter; total P accumulated in shoot; phosphorus uptake only from fertilizer; and use of fertilizer by rice plants grown in a sandy soil submitted to addition of super triple phosphate (STP), phosphate rock (P rock), or bone materials treated by calcination (O_2) or pyrolysis in sealed chamber or steam activation (WV). Letters on the columns indicate treatment difference by Tukey's test ($p \leq 0.05$) and bars are the standard error of the mean.

Results for clayey soil denotes the importance of buffering capacity at dissolving P hydroxyapatite contained in bone char. As cited above, regarding P bone char use, 400 °C was superior than other bone treatments (charred bone and calcination) together with P rock and STP almost double than other bone treatments.

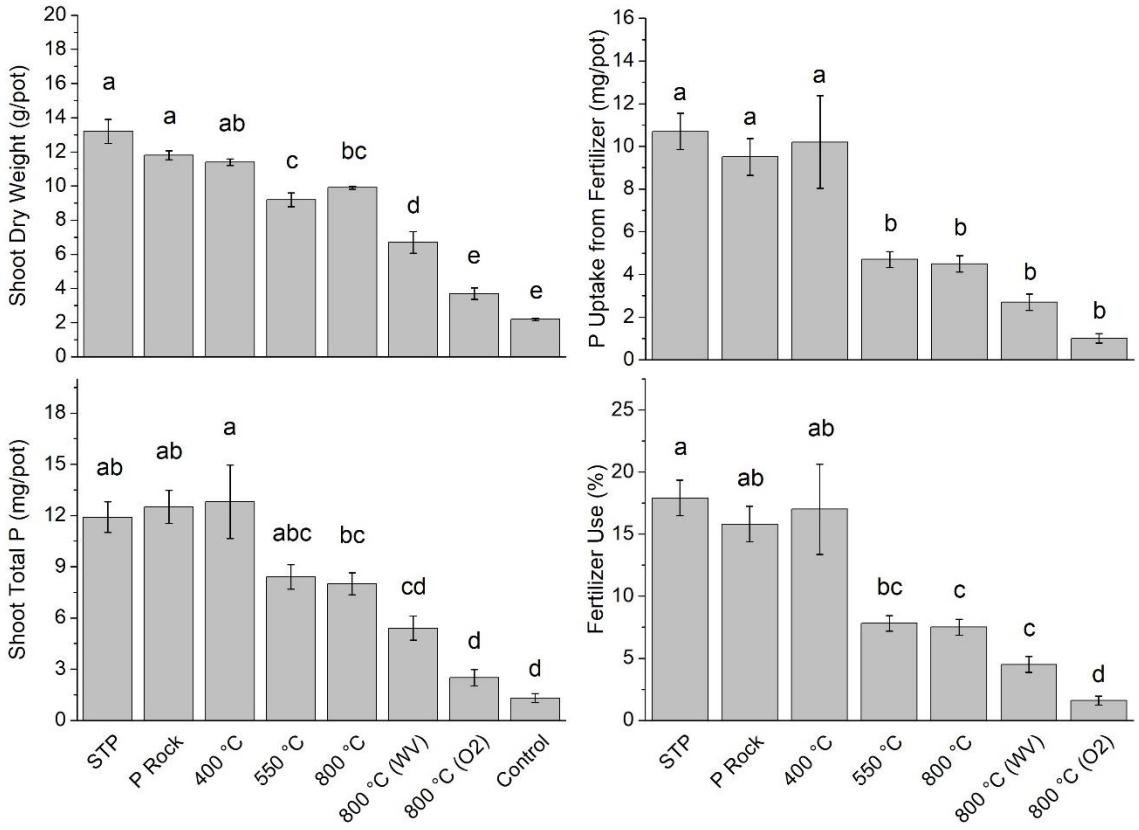

Figure 2.4 Shoot dry matter; total P accumulated in shoot; phosphorus uptake only from fertilizer; and use of fertilizer by rice plants grown in a clayey soil submitted to addition of super triple phosphate (STP), phosphate rock (P rock), or bone materials treated by calcination (O_2) or pyrolysis in sealed chamber or steam activation (WV). Letters on the columns indicate treatments difference by Tukey's test ($p \leq 0.05$) and bars are the standard error of the mean.

The lower total P (basis utilized for the calculation of P applied per kilogram of soil) contained in 400 °C resulted in an increased volume and particles of fertilizer applied. This fact also could result in increased fertilizer use due to the better distribution in the pots used for cultivation. Once P reaches to plant roots mainly by diffusion, it is important to consider this factor in studies involving materials with different P amount.

2.4. Conclusion

Pyrolysis showed to be an efficient alternative to substitute calcination as a bone treatment. The fertilizer use and amount of P absorbed by plants was higher in bone chars compared with calcined bones and bone char produced in sealed chamber at 400 °C gave the maximum values for these variables compared with all bone fertilizers produced at 800 °C.

The excessively low P dissolution rates of calcined bone verified in the stirred-chamber experiment revealed that they are not adequate to provide P to plants, as already revealed by

characterization analysis in chapter 1. Bone chars produced at temperatures as low as 400 °C in sealed chamber could substitute soluble and reactive P-rock fertilizers for application in acidic high-P fixing soils once their effect on plant growth and P absorption was equivalent to the conventional fertilizers evaluated (P rock and STP).

We suggest that bone treatment technology need to be adapted for producing more effective bone-based fertilizers, mainly when they are applied in high-P fixing soils where the fertilizer efficiency is low.

References

ÁVILA, M.P. **Influência do silício sobre a difusão do fósforo no solo e na eficiência agronômica de fertilizantes fosfatados granulados**. Masters dissertation. Universidade de Sao Paulo. 2016, 101 p.

HAVLIN, J.L., J.D. BEATON, S.L. TISDALE AND W.L. NELSON. Soil Fertility and Fertilizers. An Introduction to Nutrient Management. Pearson Education, Inc., Upper Saddle River, New Jersey. 2005.

JACKSON, M.L. **Soil Chemical Analysis**, Prentice-Hall of India Pvt. Ltd., New Delhi, India. 1973.

MARCANTE, Nericlenes Chaves. **Eficiência de absorção e utilização de fósforo por diversos cultivares de arroz e feijão do Brasil**. 2015. Doctoral thesis, Universidade de São Paulo, 2015.

MURPHY, J.; RILEY, J.P. A Modified Single Solution Method for the Determination of Phosphate in Natural Waters. **Analytica Chimica Acta**, v. 27, 1962.

RAIJ, B. van; CANTARELLA, H.; QUAGGIO, J.A.; FURLANI, A.M.C. (Ed.). **Recomendações de adubação e calagem para o Estado de São Paulo**. 2. ed. Campinas: Instituto Agronômico, 1997. 285 p.

ROY, E. D.; RICHARDS, P. D.; MARTINELLI, L. A.; COLETTA, L. Della; LINS, S. R. M.; VAZQUEZ, F. F.; WILLIG, E.; SPERA, S. A.; VANWEY, L. K.; PORDER, S. The phosphorus cost of agricultural intensification in the tropics. **Nature Plants**, v. 2, n. 5, p. 16043, 2016.

SPARKS, D.L.; ARAI, Y. Phosphate reaction dynamics in soils and soil components: a multiscale approach. **Advances in Agronomy**, v. 94, p. 135-179, 2007.

VOSE, P.B. **Introduction to nuclear techniques in agronomy and plant biology**. London: Pergamon Press, 1980. 391 p.

WANG, T.; CAMPS-ARBESTAIN, M.; HEDLEY, M.; BISHOP, P. Predicting phosphorus bioavailability from high-ash biochars. **Plant and Soil,** Dordrecht**,** v. 357, n. 1/2, p. 173-187, Aug 2012.

WARREN, G. P.; ROBINSON, J. S.; SOMEUS, E. Dissolution of phosphorus from animal bone char in 12 soils. **Nutrient Cycling in Agroecosystems**, v. 84, n. 2, p. 167–178, 2009.

ZWETSLOOT, M. J.; LEHMANN, J.; SOLOMON, D. Recycling slaughterhouse waste into fertilizer: How do pyrolysis temperature and biomass additions affect phosphorus availability and chemistry? **Journal of the Science of Food and Agriculture**, v. 95, n. 2, p. 281–288, 2015.

3. BIOCHAR AS A TOOL TO ENHANCE PLANT GROWTH IN A SOIL WITH LOW PHOSPHORUS CONTENT: THE SYMBIOTIC PATHWAY

Abstract

Biochar, a product obtained from pyrolysis of organic materials, could support plant symbiotic interactions with arbuscular mycorrhizal fungi (AMF), thus increasing plant growth in low fertility soils. Our objective was to evaluate the effect of the addition of two contrasting biochars to soil on AMF spore germination, plant-AMF symbiosis, plant growth and nutrient uptake. *Gigaspora margarita* AMF fungi spore germination was evaluated in two germination media (soil and sand) in order to verify the effect of biochar in media with contrasting buffer capacities. Biochars produced from wood chips pyrolysis at 300 and 700 °C were applied to soil that contained or not AMF inoculant, and plants were harvested after four or eight weeks of cultivation. We visualized that 700 °C biochar increased hyphae length in germinated spores in soil media, whereas biochar 300 °C inhibited germination in both media. Biochar produced at 700 °C increased soil pH, diminished toxic aluminum, augmented plant root growth and elongation and nutrient uptake, suggesting that an ameliorated root system increased plant colonization by AMF (symbiosis) and consequently plant nutrient uptake and growth. We attributed the lack of effect of biochar 300 °C on plant symbiosis and growth to the low ash and nutrient content of this biochar.

Keywords: AMF spore germination; Charred biomass; Tropical soils

3.1. Introduction

The insufficient application of nutrients through fertilizers in cultivated soils might result in low crop yield and soil covering, deforestation and land degradation. Data collected by FAO reveals the insufficient use of nitrogen, phosphorus and potassium fertilizers in most tropical regions (NATIONS, 2014), mainly those where small-scale agriculture predominates. Oppositely, an excessive fertilizer application rate is verified in countries such as China, Vietnam and Singapore. According to Peter Vitousek et al., (2009), a solution to increase crop grain yield in the cited zones could be to better distribute fertilizers in a global scale. However, we argue that the use of local resources to restore or enhance soil fertility would better suit the real conditions of small-medium scale agriculture in emergent nations around the world. Utilizing local available resources could allow farmers to attain more immediate results in terms of crop productivity in face of the difficulty to obtain manufactured fertilizers. Some countries, for example, have fertilizer access restrictions imposed either by internal/external commercial barriers or by lack of transportation facilities.

The case of phosphorus is critical, since it is a macronutrient for plants and humans and most soils have low P content in their composition, being generally the limiting element to plant growth. Accelerated weathering of soils located in tropical zones lead to the formation of Fe and Al (oxi)hydroxides in their mineral fraction, which strong affinity with ions phosphate makes most P applied as fertilizer unavailable to plants (HAVLIN et al., 2005). Additionally, low pH, nutrient and organic matter content allied to the presence of aluminum (Al^{3+}) in soil solution inhibits plant root growth. The risks associated with food security is of a big concern of the scientific community because economically phosphate rock reserves will last for up to around 80 years considering the current mineable technology (USGS, 2010).

Arbuscular mycorrhizal fungi (AMF) are ubiquitous in soils and are well-known to establish a symbiotic interaction with around 80% of plants (SMITH; READ, 1997). The symbiosis provides to fungi photoassimilates from the host plant and in exchange plant obtains water and nutrients. Fungi hyphae penetrates into the root cortex (phenomenon called colonization) and spread into the soil accessing pores and distances not accessible by roots. However, the interaction between plant roots and AMF inoculum sources (spores, hyphae and dead infected roots) depends on their proximity once AMF need to detect released signaling substances from roots, phenomenon that occurs mainly under stressful conditions. Symbiotic interactions are important tools for plants to access phosphorus and other nutrients in soils that lack in fertility and plants are also benefited by Al toxicity alleviation. Soils with low fertility

are distributed mainly in tropical regions that presents weathered and acidic soils. These soils contains Al minerals that releases Al^{3+} through dissolution, limiting root growth and colonization by AMF fungi (SIQUEIRA; HUBBELL; MAHMUD, 1984). Spore germination of AMF is not affected by pH itself, but due to the availability of toxic elements verified in soils with low pH. Because AMF is ubiquitous in soils around the world, agricultural practices that creates a better environment for AMF-plant interaction could enhance plant production in acidic soils with low phosphorus (and other nutrients) content.

Liming and organic materials (fertilizers, manures, plant residues) addition are well-known practices that could enhance soil fertility. Biochar is an organic material generated from pyrolysis of vegetal or animal by-products and could create the needed environment to form mycorrhiza (term given to the structure formed in the interface of plant root and AMF hyphae). There are only few studies showing biochar influence on plant-AMF symbiosis and no information regarding its effect on AMF spore germination was documented (WARNOCK et al., 2007). Previous studies showed that biochar addition enhanced root colonization by AMF; however, the extension of the benefits depends on biochar quality and application rate (WARNOCK, 2009). Some kinds of biochar may contain potentially toxic compounds formed during pyrolysis that could potentially damage plant roots and organisms, thus inhibiting mycorrhiza formation (KIBET; KHACHATRYAN; DELLINGER, 2012; CHEN; ZHENG; WANG, 2013).

Generally, the lower the pyrolysis temperature, the greater content of less recalcitrant compounds (volatile matter) and tar in biochar. It is not well understood if such compounds can act as a carbon source and have positive effects on plant-AMF interaction or cause toxicity to AMF and/or plants as well as restrict soil nutrient (specially nitrogen and heavy metals, such as Mn, Cu and Zn) availability due to their immobilization (DEENIK et al., 2010). On the other hand, high temperature biochars (>500 °C) shows greater pH, ash and nutrient content compared to materials obtained at lower temperatures. Such materials are more recalcitrant and less reactive with polar molecules in soils and show an increased porosity, which can act as AMF shelter (SAITO, 1990; ENDERS et al., 2012). Moreover, AMF hyphae can extract phosphorus from biochar pores (HAMMER et al., 2014) and this could contribute to increase P uptake of plants colonized by AMF.

Biochar use for promoting plant interaction with AMF could enhance plant growth, thus support farmers that have limited or no access to manufactured fertilizers. We hypothesize that the temperature of pyrolysis drives biochar responses on plant-AMF symbiosis and plant growth. Our aim was i) to verify the effect of contrasting biochars regarding temperature on

AMF spore germination; ii) evaluate biochar capability to improve plant-AMF symbiosis, plant growth and nutrient absorption.

3.2. Material and Methods

3.2.1. Biomass pyrolysis

Pyrolysis was performed at the Integrated Laboratory of Chemistry, Cellulosis and Energy at University of São Paulo, Brazil. Eucalyptus woodchips were chosen as a feedstock since the resultant biochar presents low ash and nutrient content and thus the effect of AMF-plant interaction on P absorption could be better verified. Biochars were produced by slow pyrolysis (heating rate of 1 °C min^{-1}) until 300 and 700°C, and 1 hour of residence time (time that the sample holds at the chosen temperature). These temperatures ensured well defined contrasting characteristics of biochars, such as volatile matter, pH, nutrient content and physical properties. Pyrolysis products yield, which corresponds to biochar, condensable and non-condensable gases (by difference), was recorded. Biochars were ground and passed through a sieve with 1 mm aperture.

3.2.2. Biochar characterization

The produced biochars were characterized by proximate analysis (moisture, fixed carbon, volatile matter and ash content) (ASTM D 1762-84, 2011); elemental C and N (LECO elemental analyzer); BET surface area, porosity and pore diameter as described by Schimmelpfennig and Glaser, (2012). For BET analysis, a pretreatment at 150 °C during 3h was utilized for degassing biochar samples before performing N_2 sorption/desorption at 77 K. Nutrients and other elements were extracted from biochar with Mehlich-III (1:100; m:v) (MEHLICH, 1984).

3.2.3. Arbuscular mycorrhizal fungi spore germination

To be effective at stablishing a symbiotic interaction with plants, AMF spores need to germinate and the formed hyphae (structure emerging from spores) must reach plant roots. In order to evaluate biochar quality influence on symbiosis between AMF and plants (given by root colonization parameter), we first tested the germination potential of AMF spores exposed to the biochars in two germination media.

Treatments included the combination of incubation media and biochar type. Treatments involved the eucalyptus biochars produced at 300 and 700 °C applied at 5 % rate (w/w) in 10 g of soil or quartz sand (germination media), plus control with no biochar addition, totalizing 24 petri dishes in a completely randomized design (Figure 3.1A). Soil, biochars and sand were sterilized in a furnace at 160 °C for 2 h. The soil, classified as Haplic Acrisol (WRB soil Taxonomy), was acidic, had low fertility, contained exchangeable Al, and 491, 409 and 100 g kg^{-1} of sand, silt and clay, respectively (sandy texture) (Table 3.1).

Soil pH and other factors, as presence of exchangeable Al, can inhibit spore germination (CLARK, 1997). Thus, we selected the AMF specie *Gigaspora margarita* due to its increased spore viability in acidic media, characteristic present in the utilized soil. It is important to notice that the inoculant utilized in the pot experiment (next section) contained *Glomus* sp. spores, which are less resistant to soil acidity than *G. margarita*. Therefore, germination promotion or inhibition provoked by biochar to *G. margarita* could better indicate the performance of the tested biochars on plant colonization by *Glomus* sp. In addition, since there is no previous reported data, the spore germination experiment employed a higher biochar application rate (5%, w/w) than in the pot experiment (1%) to facilitate a possible biochar effect on spore germination. Moreover, field application of any organic residue is generally performed on the top soil layer with no or little incorporation of the material, increasing local concentration of biochar in the soil.

Table 3.1 Characteristics of the sandy soil used in the pot experiment.

P	S	B	Cu	Fe	Mn	Zn	K	Ca	Mg	Al	H+Al	SB	CEC	pH	V	m	OM
mg dm^{-3}							$mmol_c$ dm^{-3}								%		
5	128	<0.2	0.1	3	0.9	0.1	0.2	12	3	5.7	28	15.2	43.2	4.2	35	27	0.4

SB: sum of bases; CEC: cation exchange capacity; V: base saturation; m: aluminum saturation in effective CEC. Extraction methods: P, Ca, Mg, K: resin; B: hot water; Fe, Cu, Mn, Zn: DTPA; Al: KCl 1 M; S: calcium phosphate 0.01 M; organic matter (OM): oxidation by dichromate in acid media. Potential acidity (H+Al) determined by pH in SMP buffer

Soil and sand mixed or not with biochars were disposed in petri dishes. According to previous tests, three and four milliliters of autoclaved (121 °C for 20 min) deionized water were added in sand and soil media, respectively, to guarantee suitable moisture conditions for spore germination.

Spores were surface disinfested by solutions containing 2% of chloramine T (solution 1), and 1% of streptomycin and gentamycin (solution 2). A small drop of the surfactant Tween 20 was added to each sterilizing solution. Subsequently, the sterilizing solution 1 containing spores was centrifuged for 60 seconds and discarded. Spores were then washed 5 times with deionized water. The same sterilizing and washing cycle was performed with the solution 2.

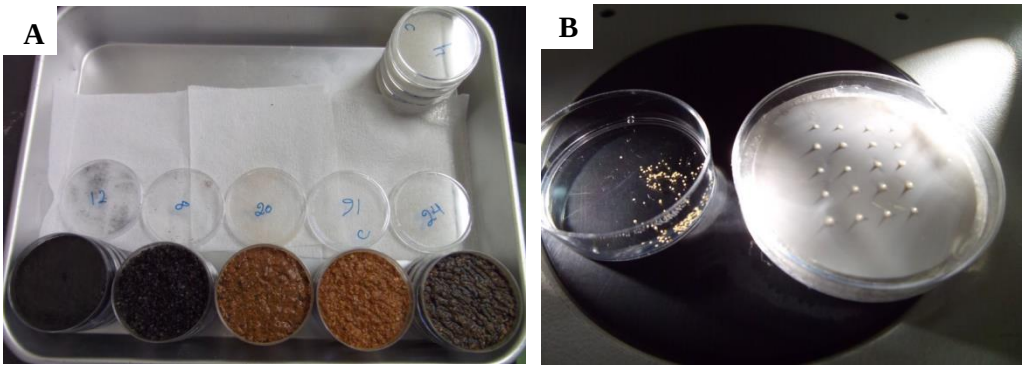

Figure 3.1 A: Soil and sand media mixed with biochar at 5% rate, after water addition. B: spores of Gigaspora margarita placed on a cellulose membrane filter for posterior incubation.

Twenty AMF spores were distributed on a moisturized 0.45 μm pore size sterile membrane filter that was previously disposed on the solid mixtures of each treatment (Figure 3.1B). There was no contact of solids with spores. After sealing the petri dishes with Parafilm®, spores were incubated at 30 °C and daily checked for germination during 2 weeks until no further germination. Spores were considered to have germinated if the length of the germ tube was equal to, or higher than the spore diameter (BRUNDRETT et al. 1996). Afterwards, media pH was measured (1:2.5, w/v).

The statistical analysis was performed by SAS® and R softwares. Analysis of variance was executed after testing its assumptions and transforming data when necessary. Tukey's test was applied to compare means ($p \leq 0.05$).

3.2.4. Growth and nutrient uptake of plants submitted to biochar and AMF inoculation

To test the effect of biochars and AMF on plant growth and nutrient extraction from soil, dwarf-sorghum plants were cultivated with or without addition of AMF, at the Laboratory of Environmental Crop Science, Kawatabi Field Center, University of Tohoku, Japan. Pots were soaked in 1% (v/v) NaOCl solution overnight, and then washed with tap water to

completely remove the sterilization solution (SAITO et al., 2011). Subsequently, pots were filled with 350 g of air-dried soil previously sterilized by autoclaving at 121 °C for 20 minutes.

Treatments comprehended: (i) addition of biochars (300 and 700°C) at 1% rate (w/w) plus control with no biochar; (ii) application of a commercial AMF inoculant containing *Glomus spp.* (Doctor Kinkon®) added at 0.5% (w/w) and control (sterilized inoculant). Potassium (K_2SO_4) and nitrogen were applied at 100 mg kg^{-1}, Ca at 143 mg kg together with the nitrogen source [$(NO_3)_2.4H_2O$] and magnesium ($MgSO_4.7H_2O$) at 10 mg kg^{-1}. Plants were daily watered to keep soil moisture content 50% of the maximum water holding capacity (0.44 g g^{-1}). In a completely randomized design, four replications each treatment applied and one plant of dwarf-sorghum was cultivated per pot in a growth chamber set to 25 °C, with a photoperiod of 14 and 10 hours of light and dark, respectively.

Plants were harvested at four and eight weeks in order to observe AMF-plant symbiosis, plant growth and nutrient uptake in different growth stages. After harvesting, plant shoot and root fresh and dry weight (65 °C for 48h) were recorded. Nutrient concentration in plant shoot was revealed by energy dispersive X-ray spectroscopy (EDS), which was measured for 300 s with a current of 240 µA. Total P and other macro (K, Ca, S) and micronutrients (Fe, Zn, Mn) absorbed by plants were calculated by multiplying nutrient content in shoot by shoot dry weight. Part of the fresh roots were cut into small pieces, cleared (KOH 10%) in water bath, stained with trypan blue and submitted to colonization measurement by the gridline intersection method (BRUNDRETT et al. 1996) under microscope. Root length was accessed by root scanning. Root length was calculated by adding up the lengths obtained in each class of root diameter (five diameter classes in total, from 0-0.1 mm to >1 mm) by using the free software ImageJ (TAJIMA; KATO, 2013). To verify soil chemical conditions that could interfere on nutrient availability, P availability (Mehlich-I), pH (1:2.5, soil:water) and Al^{3+} were analyzed in the soil collect from the pots (BERTSCH; BLOOM, 1996).

Analysis of variance and Tukey's test was performed similarly to the pot experiment, described above. We considered the group of plants harvested at four and eight weeks as two different experiments since they were independent from each other and tested the main, and interaction of factors (biochar temperature *versus* inoculation).

Principal component analysis (PCA) was carried out for plants harvested at eight weeks to better characterize our treatments. The identification of the most relevant variables among several (Ca, Mn, Al, pH, Zn, P, K, S and Fe for soil and SDM, RDM and RL for plants) may facilitate the explanation of processes associated with treatments applied to the soil. Pearson's

correlation was employed to reveal the relationship between colonization data with other analyzed variables.

3.3. Results and Discussion

3.3.1. Pyrolysis products yield and biochar characteristics

Pyrolysis causes degradation of less thermal-stable compounds and elements that are released as gas. Our data showed that biochar yield decreased when temperature rose from 300 to 700 °C (Table 3.2). Because mass loss is increased at 700 °C, the amount of condensable and non-condensable gases is greater in this biochar temperature. Most part of volatiles can be condensed, which could diminish environmental impacts of pyrolysis. The condensed gas fraction as well as syngas (also produced during pyrolysis) could be utilized as combustible, for example (SOHI et al., 2010).

Table 3.2 Pyrolysis products yield of biochars produced in two different temperatures

Temperature	Biochar	Condensable gases	Syngas
		%	
300 °C	77.5	13.6	8.9
700 °C	30.9	43.8	25.3

Biochar produced at 300 °C showed around 7- fold higher volatile matter and 3-fold lower fixed carbon (more stable fraction) content than 700 °C biochar (Table 3.3). Volatile matter can be responsible for pore trapping in 300 °C biochar due the its lower pore diameter given by BET analysis. Porosity and surface area of biochar 700 °C were respectively 25- and 32-fold higher than biochar obtained at 300 °C as a result not only of pore blockage by organic volatiles in the latter, but also due to matter degradation and development of porous in the carbonaceous matrix in the first during pyrolysis (SUN et al., 2012).

Carbon increased from 58 to 92% when pyrolysis rose from 300 to 700 °C due to the increased loss of other compounds as structural water, and O, H, S and N compounds, which are lost at lower temperatures (SPOKAS et al., 2011). Nitrogen content is negligible (≤ 0.2 %) and once an optimal C/N ratio between 20-30 would be needed to inhibit excessive C mineralization and N immobilization in soils, both biochars could immobilize N in soils and negatively affect plant growth. However, 300 °C biochar increased volatile matter content

would provoke a higher N immobilization because volatiles could be degraded by microorganisms (consuming soil N), in opposite to the highly aromatic structure contained in biochar 700 °C.

Ash content and consequently solubility (Mehlich-III) of elements that starts to volatilize at temperatures above 600 °C such as K, P, Ca and heavy metals (DE LUCA et al., 2009) increased in biochar produced at 700 °C (Table 3.4). As a consequence, biochar pH increases since basic cations in ash are mainly in oxide form (e.g. CaO, MgO) that neutralizes soil acidity as they dissolve (TRIPODI; CHEREMISINOFF, 1980) (Table 3.3). Both eucalyptus biochars had low ash (and thus nutrient) content compared to biochars produced from materials such as manure and straw (ZHAO; CAO, 2013). This explains the slight differences in extractable elements between the two biochars, except for K that was 2-fold higher in 700 °C biochar. Soluble sodium in Mehlich-III is present in quantities comparable to potassium, mainly because *Eucalyptus spp.* can substitute K by Na in metabolism. Clay dispersion might occur when Na is applied in excessive rates, causing soil compaction, erosion and other related issues, but even at application rates around 20 tons per hectare, which equal to the rate utilized in the pot experiment (considering a soil layer of 20 cm) would not be enough to provoke the cited issues once the Na input calculated from Mehlich-III results would be 3.18 kg ha^{-1}. Silicon shows the highest content in ash fraction among the evaluated elements in biochar, mainly because soils are composed by silicon-rich minerals (SPARKS, 1995).

Table 3.3 Proximate analysis results; total carbon and nitrogen; C/N ratio and pH; and physical properties of the produced biochars.

Temperature	Moisture	VM	Fixed C	Ash	C	N	C/N	pH	Porosity	PD	SA
	%						-		$cm^3\ g^{-1}$	Å	$m^2\ g^{-1}$
300 °C	3.8	69.2	26.6	0.4	58.5	0.03	1690	5.9	0.002	29.4	1.7
700 °C	5.5	10.1	83.5	1.0	92.5	0.2	523	8.3	0.05	17.8	55.2

VM: volatile matter; PD: pore diameter; SA: surface area.

Table 3.4 Biochar elements extracted by Mehlich-III

Temperature	P	K	Ca	Mg	S	Fe	Cu	Zn	Mn	B	Si	Na	Al
	$mg\ kg^{-1}$												
300°C	1.8	56.1	117.4	17.5	4.5	3.6	0.1	0.3	3.5	0.3	460.1	157.1	21.2
700°C	2.8	117.9	136.4	18.1	5.2	4.3	0.1	0.5	4.0	0.8	471.8	159.0	24.3

3.3.2. Arbuscular mycorrhizal fungi spore germination

Because the highest germination of *G. margarita* spores occurs around pH 6 (SIQUEIRA; HUBBELL; MAHMUD, 1984), sand (pH=6) with no biochar application was considered the overall control of the experiment, while soil (pH=4.2) without biochar addition was control only for soil media.

Spore germination in soil media was 62% when 700 °C biochar was applied, while a decrease to 1 and 10% in germination was verified for control and 300 °C biochar. The spore germination of the control in sand media was 58%, whereas 700 °C and 300 °C biochars diminished to 10 and 11%, respectively (Fig. 3.2).

Biochar 700 °C in soil media was the only treatment that caused a spore germination equivalent to control in sand media. The probable cause of this result is the pH, which increase from 4.7 in soil with no biochar addition (10% of germination) to 5.4 (Fig. 3.3). In addition, nutrients provided through the addition of 700 °C biochar and the higher aromaticity (and nonpolar adsorption potential) compared to a 300 °C biochar (SINGH; SINGH; COWIE, 2010), are suggested to have enhanced nutrient availability and/or adsorbed germination inhibitory compounds that were present in the soil (WARNOCK et al., 2007). We also visualized an increased hyphae length in the spore germinated in soil under addition of 700 °C and the production of 29, 21, 12 and 9 auxiliary cells (structures that functions are still not well understood and present in only some AMF species) each petri dish, indicating improving effects of this biochar on the growth of *G. margarita* (Figs. S3.1 and S3.2).

We attributed the germination inhibition caused by 700 °C biochar in sand media to the pH, which rose to 9.5 as a result of the negligible buffer capacity of sand that could also permit a toxic effect by the elements present in biochar ash fraction. For 300 °C biochar, the pH did not change when compared to control sand media treatment. However, spore germination in both media decreased to <11%, suggesting that volatile compounds present in low temperature biochars are toxic to spores, similarly to seeds (BUSS, 2014; SPOKAS et al., 2011).

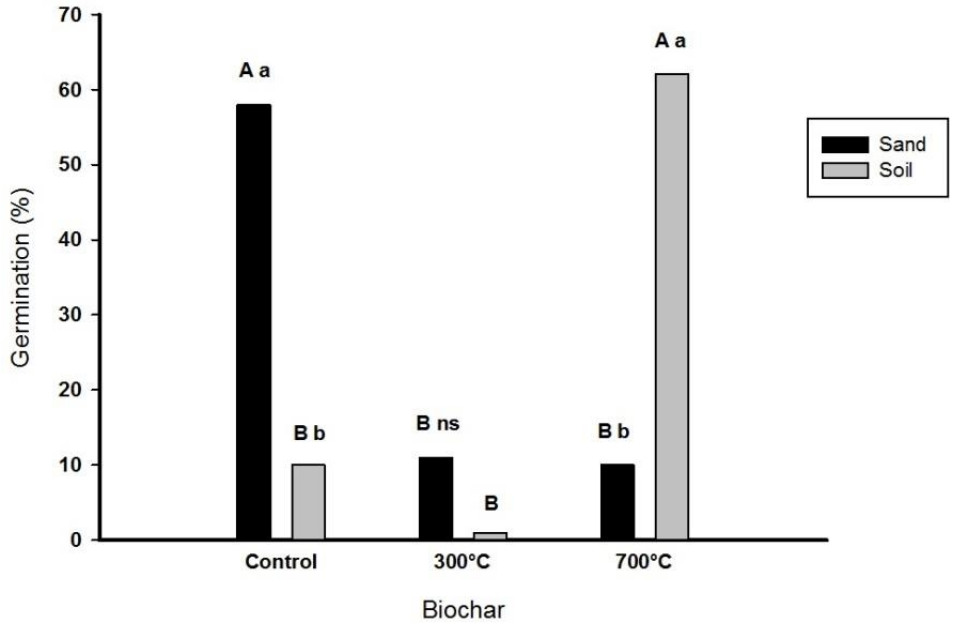

Figure 3.2 Germination percentage of the interaction analysis of biochar type with media (soil and sand). Uppercase letters compare biochar and lowercase letters compare media by Tukey's test ($p \leq 0.05$).

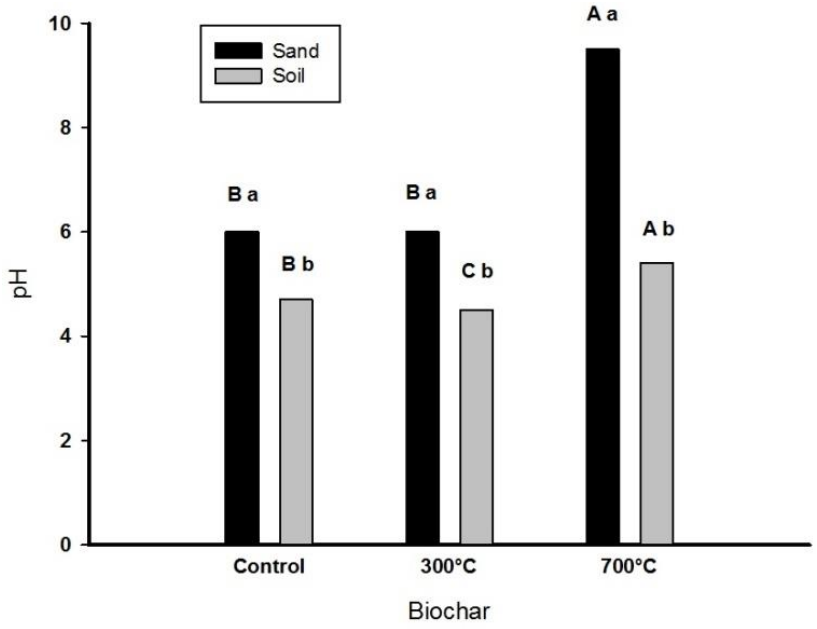

Figure 3.3 Values of pH in the interaction between biochar and spore germination media factors. Uppercase letters compare biochar in the same media level. Lowercase letters compare media in the same biochar level by Tukey's test ($p \leq 0.05$).

3.3.3. Growth and nutrient uptake of plants submitted to biochar and AMF inoculation

The percentage of roots colonized by AMF was <5% in both harvesting periods for control and 300 °C biochar treatments, while plants submitted to the addition of 700 °C biochar

showed a root colonization of <10% and 65% for plants harvested at four and eight weeks, respectively (Figure 3.4). The greater colonization of plants submitted to 700 °C biochar might be due to an increased root length verified at eight weeks of cultivation (Table 3.6). Root colonization is more probable to occur when roots are longer, once signaling compounds released from roots (of plants generally under stressful conditions) must be detected by fungi (OLDROYD, 2013). Colonization was low in control and 300 °C biochar treatments and seemed to be a response of low soil fertility and root elongation. Colonization is important in soils with low fertility; however, our results suggest that the addition of a source of nutrients as ash-rich materials as 700 °C is important to promote plant colonization, possibly impacting on the increase of plant growth.

Plant shoot and root dry matter were similar for all treatments at four weeks (except for 300 °C that showed lower dry matter in non-inoculated plants), possibly due to the low soil fertility, which slowed down the early phase of plant growth (Tables 3.5 and 3.7). Because of the low fertility of the soil used in the study (control), suppressive effects of 300 °C biochar on plant growth might have been hindered. For plants harvested at eight weeks, the greatest plant shoot and root dry weight was verified for the 700 °C treatment, whereas 300 °C biochar plants showed values equivalent to the control. There was no interaction between inoculation and biochar temperature factors for all variables, except for root dry weight, where inoculated plants showed at eight weeks lower root dry weight when inoculated. Although the colonization was low in the control treatment, AMF might have competed with plants for water and nutrients, diminishing plant root growth.

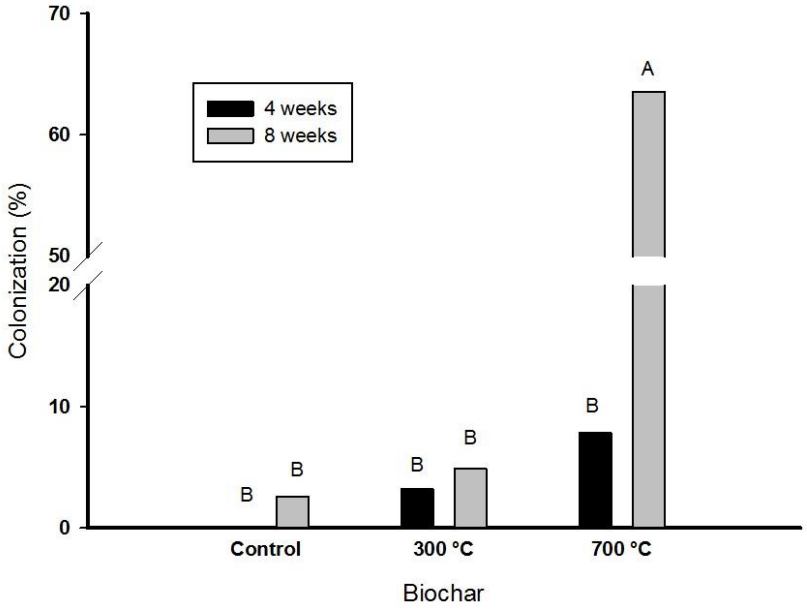

Figure 3.4 Root colonization by arbuscular mycorrhizal fungi of plants harvested at four and eight weeks, submitted to the addition of biochar. Means for Tukey's test ($p \leq 0.05$). Letters compare biochar in the same harvesting period.

The root length of plants from 700 °C biochar treatment increased 2.7-fold from four to eight weeks of harvesting and was at the second harvesting period ~4-fold higher than 300 °C biochar and control treatments, which showed no root length increase between the two harvesting periods. Regarding root diameter, which is important to nutrient uptake, in both harvesting periods plants submitted to biochar 700 °C had 48% of total root length composed by roots with a diameter <0.2 mm, whereas non-inoculated plants had 35% (Table 3.8). This reinforce the effectiveness of 700 °C biochar at promoting plant nutrient absorption and growth.

Pearson's correlation between plant colonization and soil pH was equal to 0.63 and 0.96 at four and eight weeks, respectively. Soil Al^{3+} was reduced as pH increased; thus, negative effects of Al^{3+} on plant growth (shoot and root dry matter weight and root length) caused by Al^{3+} presence were possibly diminished (Tables 3.5 and 3.6). In addition, plant-AMF symbiosis might also support plant growth due to Al^{3+} toxic effects alleviation (LOUVAIN; UNITE; CROIX, 2000). Therefore, the increased shoot and root dry matter and root length of plants cultivated under 700 °C could be addressed to biochar increased ash (and nutrient) content and its liming effect (pH rise) that was observed within the first four weeks of cultivation. Moreover, soil liming effect promoted by high ash biochar addition also enhances nutrient availability in soils, which could have improved plant growth.

Plants from 700 °C biochar treatment at 8 weeks of harvesting showed 5-fold higher P uptake compared to 300 °C biochar (Table 3.7), phenomenon that we attributed to the increased soil pH and its effects at enhancing root dry weight and length, as discussed above. Although

the P uptake for this treatment was augmented, plants also showed purple colored leaves as a result of the well-known P deficiency symptom. All plant leaves started becoming purple within the first month of cultivation as a result of P deficiency. We observed that at 40 days after germination plants cultivated under inoculation with AMF and treated with biochar 700 °C started to turn green from purple (Figure S3.3). It suggests the beginning of the symbiosis effectiveness in overcoming P deficiency in plants in such experimental conditions. Although no statistical interaction between biochar and inoculation factors was detected by Tukey's test ($p \leq 0.05$), the visual evidence of deficiency overcoming indicates the contribution of symbiosis in plant growth and nutrient (mainly P) uptake. The P is commonly a critical element for plant development once it is required in high amounts by plants (macronutrient) and has low diffusion rate in soils. Tropical zones, which soils are highly weathered and shows low P content, P deficiency in plants is even more serious (HAVLIN et al., 2005). Symbiosis with AMF helps plants to overcome nutrient deficiency symptoms, but these fungi might sometimes be competitors when the nutrient level in soil is below plant requirements and cause plant growth suppression (in Table 3.7, inoculated plants showed lower root dry weight at eight weeks than non-inoculated plants) (CLARK; ZETO, 2000). Plant grow was not limited by nutrients other than P since we compared the concentration of the evaluated nutrients in our samples were within the range values reported for non-deficient plants (RAIJ et al., 1997). Biochar 700 °C also increased K, S and Zn accumulation in plants harvested at eight weeks (Table 3.6).

Table 3.5 Shoot dry weight, root length and total P content in shoot of dwarf-sorghum plants along with soil exchangeable aluminum and pH after addition of biochar and inoculation with arbuscular mycorrhizal fungi. Plants harvested after four weeks of cultivation.

Treatments	Shoot DW	Root Length	P	Soil Al^{3+}	Soil pH
	g	Cm	µg/pot	$mmol_c\ kg^{-1}$	
300 °C	0.06 ns	70.8 b	11.0 ns	6.5 a	4.4 b
700 °C	0.07	135.2 a	12.0	3.9 c	4.7 a
Control (no biochar)	0.06	112.6 ab	10.5	5.8 b	4.4 b
Inoculated	0.06 ns	93.5 ns	11.0	0.3 ns	4.5 ns
Non-inoculated	0.07	117.4	11.4	0.3	4.5

Letters mean statistical significance by Tukey's test ($p \leq 0.05$). ns: non-significant; DW: dry weight.

Table 3.6 Shoot dry weight, root length and total nutrient content in shoot of dwarf-sorghum plants along with soil exchangeable aluminum and pH after addition of biochars and inoculation with arbuscular mycorrhizal fungi. Plants harvested after eight weeks of cultivation.

Treatments	Shoot DW	Root Length	P	S	Zn	K	Soil Al^{3+}	Soil pH
	g	cm	µg/pot			mg/pot	$mmol_c\ kg^{-1}$	
300 °C	0.115 b	87.2 b	7 b	161.1 b	2.1 b	1.1 b	5.8 a	4.4 b
700 °C	0.187 a	363.1 a	35 a	240.4 a	3.6 a	2.9 a	3.5 b	4.8 a
Control (no biochar)	0.108 b	88.6 b	5 b	158.9 b	2.0 b	1.0 b	5.6 a	4.4 b
Inoculated	0.131 ns	197.9 ns	26 a	184.5 ns	2.5 ns	1.7 ns	4.9 ns	4.6 ns
Non-inoculated	0.143	161.4	6 b	189.1	2.7	1.6	5	4.5

Letters mean statistical significance by Tukey's test ($p \leq 0.05$). ns: non-significant. DW: dry weight

Table 3.7 Root dry weight of dwarf-sorghum plants cultivated under addition of biochar produced at 300 °C and 700 °C in media inoculated or non-inoculated with arbuscular mycorrhizal fungi, harvested at four or eight weeks.

Biochar	Root Dry Weight (g)	
	Inoculated	Non-inoculated
	4 weeks	
300 °C	0.022 NS ns	0.014 B
700 °C	0.021 ns	0.030 A
Control	0.018 ns	0.033 A
	8 weeks	
300 °C	0.020 B ns	0.033 B
700 °C	0.085 A ns	0.072 A
Control	0.019 B b	0.034 B a

Uppercase letters compare biochar and lowercase compare inoculation by Tukey's test ($p \leq 0.05$), which employed transformed variables [$\log_{10}$(variable)]. The represented mean values were back-transformed.
ns: non-significant

Table 3.8 Contributing percentage of each root diameter class in total root length of plants submitted to addition of biochars and inoculation with arbuscular mycorrhizal fungi (results not tested by ANOVA).

Treatment	Inoc	0-0.1mm	0.1-0.2mm	0.2-0.5mm	0.5-1.0mm	>1.0mm
		%				
300 °C		11	13	26	26	25
700 °C		19	22	33	16	12
Control		9	15	29	27	20
	Inoc	15	19	28	21	17
	Non-inoc	12	14	30	24	20
300 °C	Inoc	11	16	28	24	22
700 °C	Inoc	23	25	29	14	10
Control	Inoc	9	15	29	27	20
300 °C	Non-inoc	11	10	25	28	27
700 °C	Non-inoc	15	18	36	18	14
Control	Non-inoc	10	15	29	28	19

As cited above, possible N deficiency due to immobilization occurred after introduction of a high C:N material in the soil was not considered once soil was sterilized (reducing bacterial activity responsible for immobilizing N), nitrogen was applied at 100 mg kg^{-1} rate (DEENIK et al., 2010) and biochars are recalcitrant, making most of their organic fraction inaccessible to microorganisms.

Principal component analysis revealed that plants cultivated under addition of biochar 700 °C and inoculation with AMF had distinguished plant growth (given by shoot and root dry matter and root length) and nutrient uptake in principal component 1 (Fig. 3.5). This analysis indicated that plant growth was more associated with plant absorption of Zn, P, K, S and Fe than Ca and Mn. On the other hand, soil from control and 300 °C biochar treatments showed increased soil exchangeable Al and lower plant growth than 700 °C treatments. Aluminum and pH clearly had an antagonistic effect. The increased ash content in biochar 700 °C augmented soil pH and decreased Al, and when associated with AMF inoculation, plants grew and absorbed more nutrients than plants cultivated in absence of AMF. Principal component 2 revealed that the treatments with inoculation, except for 700 °C biochar, resulted in higher Ca and Mn absorption by plants than non-inoculation.

Principal component 1 analysis suggests also that the addition of AMF caused positive effects on plant growth and nutrient absorption only when 700 °C biochar was applied, mainly because root colonization was 65% and this biochar provided nutrients to soil. On the other hand, treatments without addition of biochar, or addition of 300 °C biochar (low nutrient content), might have caused a competition between plants and AMF even when roots had a colonization of <10%.

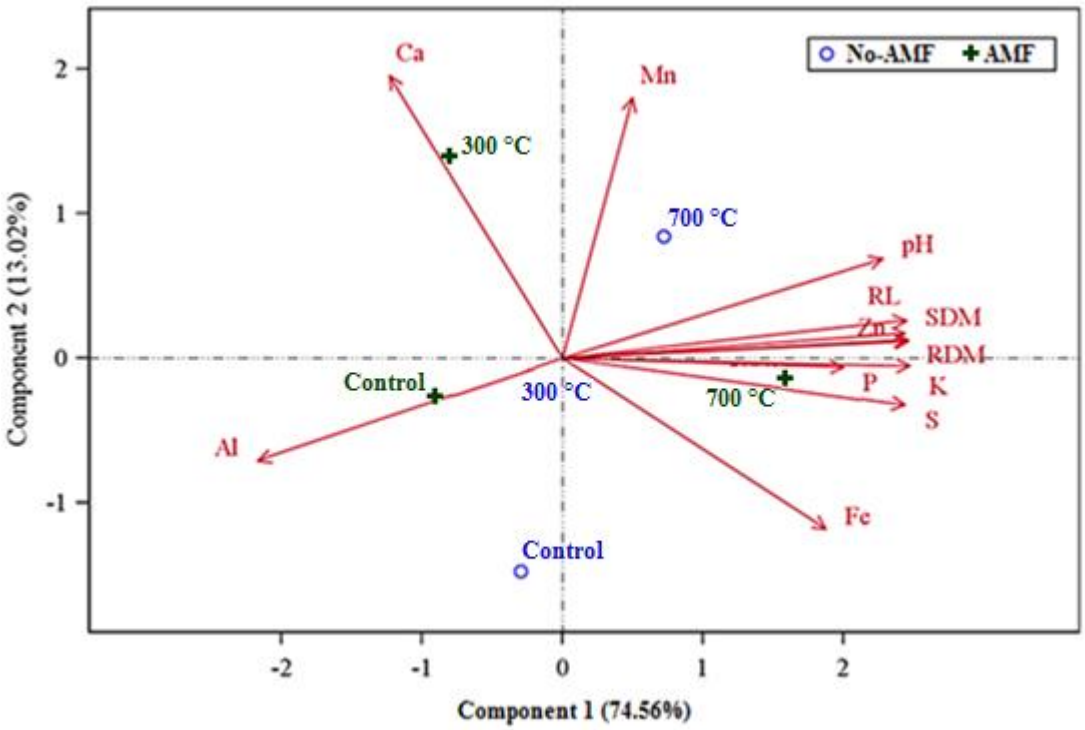

Figure 3.5 Principal component analysis of variables evaluated in soil and plants submitted to the addition of two biochars (300 and 700 °C) plus control (no biochar) and inoculation with arbuscular mycorrhizal fungi. AMF: soil inoculated with AMF; No-AMF: non-inoculated; Al: exchangeable aluminum in soil; pH: soil pH; SDM: shoot dry matter; RDM: root dry matter; RL: root length. Other chemical symbols represent the total of each nutrient (Ca, Mn, Zn, P, K, S, Fe) absorbed by plant shoot per pot.

3.4. Conclusion

Our results demonstrated that pyrolysis temperature alters biochar quality and its effect on plant growth, nutrient uptake and AMF spore germination. Biochar produced at 700 °C increased plant growth and nutrient absorption and such phenomena seems to rely on the amelioration of soil fertility (acidity reduction and addition of nutrients) and promotion of plant symbiotic interaction with AMF. Contrarily, addition of 300 °C biochar to soil do not change plant growth and nutrient uptake. A spore germination test in petri dish suggests that 300 °C biochar inhibits AMF spore germination, but when plants were submitted to the addition of this biochar, no differences in terms of root colonization by AMF were detected.

References

ASTM D 1762-84. Standard Test Method for Chemical Analysis of Wood Charcoal. **ASTM International**, v. 84, n. Reapproved 2007, p. 1–2, 2011.

ATKINSON, C. J.; FITZGERALD, J. D.; HIPPS, N. A. Potential mechanisms for achieving agricultural benefits from biochar application to temperate soils: a review. **Plant and Soil,** v. 337, n. 1-2, p. 1-18, 2010.

BEESLEY, L.; BEESLEY, L.; MORENO-JIMÉNEZ, E.; GOMEZ-EYLES, J. L.; HARRIS, E.; ROBINSON, B.; SIZMUR, T. A review of biochars' potential role in the remediation, revegetation and restoration of contaminated soils. **Environmental Pollution,** v. 159, n. 12, p. 3269-3282, 2011.

BLAKEMORE, L.C.; SEARLE, P.L.; DALY, B.K. **Methods for Chemical Analysis of Soils**. New Zealand Soil Bureau Scientific Report 80, 1987, 103 p.

BRUNDRETT M, BOUGHER N, DELL B, GROVE T, MALAJCZUK N. **Working with Mycorrhizas in Forestry and Agriculture**, ACIAR Monograph 32, p. 179–187. ACIAR, Canberra, 1996.

BUSS, W. Mobile organic compounds in biochar - A potential source of contamination - Phytotoxic effects on cress seed (Lepidium sativum) germination. **Journal of Environmental Management**, v. 137, p. 111–119, 2014.

CHEN, L.; ZHENG, H.; WANG, Z. The Formation of Toxic Compounds during Biochar Production. **Applied Mechanics and Materials.** v. 363, p. 867–870, 2013.

CLARK, R. B. Arbuscular mycorrhizal adaptation, spore germination, root colonization, and host plant growth and mineral acquisition at low pH. **Plant and Soil**, v. 192, n. 1, p. 15–22, 1997.

CLARK, R. B.; ZETO, S. K. Mineral acquisition by arbuscular mycorrhizal plants. **Journal of Plant Nutrition**, v. 23, n. 7, p. 867–902, 2000.

DEENIK, J. L.; MCCLELLAN, T.; UEHARA, G.; ANTAL, M. J.; CAMPBELL, S. Charcoal Volatile Matter Content Influences Plant Growth and Soil Nitrogen Transformations. **Soil Science Society of America Journal**, v. 74, n. 4, p. 1259, 2010.

DE LUCA, T.Hl.; MACKENZIE, M.D.; GUNDALE, M.J. Biochar effects on soil nutrient transformations. In: LEHMANN, J.; JOSEPH, S. Biochar for environmental management: science and technology. London: Earthscan,. n. 14, p. 251–270, 2009.

ELAD, Y., CYTRYN, E., HAREL, Y. M., LEW, B., & GRABER, E. R. The Biochar Effect: plant resistance to biotic stresses. **Phytopathologia Mediterranea,** v. 50, n. 3, p. 335-349, 2011.

ENDERS, A.; HANLEY, K.; WHITMAN, T.; JOSEPH, S.; LEHMANN, J. Characterization of biochars to evaluate recalcitrance and agronomic performance. **Bioresource Technology**, v.

114, p. 644–653, 2012.

HAMMER, E. C.; BALOGH-BRUNSTAD, Z.; JAKOBSEN, I.; OLSSON, P. A.; STIPP, S. L. S.; RILLIG, M. C. A mycorrhizal fungus grows on biochar and captures phosphorus from its surfaces. **Soil Biology and Biochemistry**, v. 77, p. 252–260, 2014.

HAVLIN, J.L., J.D. BEATON, S.L. TISDALE AND W.L. NELSON. **Soil Fertility and Fertilizers**. **An Introduction to Nutrient Management**. Pearson Education, Inc., Upper Saddle River, New Jersey, 2005.

KIBET, J.; KHACHATRYAN, L.; DELLINGER, B. Molecular products and radicals from pyrolysis of lignin. **Environmental Science and Technology**, v. 46, n. 23, p. 12994–13001, 2012.

LEHMANN, J., RILLIG, M. C., THIES, J., MASIELLO, C. A., HOCKADAY, W. C., & CROWLEY, D. Biochar effects on soil biota - A review. **Soil Biology & Biochemistry,** v. 43, n. 9, p. 1812-1836, 2011.

LOUVAIN, U. T. De; UNITE, T.; CROIX, P. Arbuscular mycorrhizal fungi might alleviate aluminium toxicity in banana plants. **Applied Soil Ecology**. p. 343–352, 2000.

MEHLICH, A. Mehlich 3 soil test extractant: A modification of Mehlich 2 extractant. **Communications in Soil Science and Plant Analysis**, v. 15, n. 12, p. 1409–1416, 1 dez. 1984.

NATIONS, F. and A. O. of the U. **FAOSTAT Fertilizers**. Rome, Italy FAO, 6 mar. 2014.

NOVOTNY, E. H., HAYES, M. H., MADARI, B. E., BONAGAMBA, T. J., AZEVEDO, E. R. D., SOUZA, A. A. D. Lessons from Terra Preta de Índios of the Amazon region for the utilisation of charcoal for soil amendment. **Journal of the Brazilian Chemical Society,** São Paulo, v. 20 n. 6, p. 1003-1010, 2009.

OLDROYD, G. E. D. Speak , friend , and enter : signalling systems that promote beneficial symbiotic associations in plants. **Nature Reviews**. v. 11, n. 4, 2013.

RAIJ, B. van; CANTARELLA, H.; QUAGGIO, J.A.; FURLANI, A.M.C. (Ed.). **Recomendações de adubação e calagem para o Estado de São Paulo**. 2. ed. Campinas: Instituto Agronômico, 1997. 285 p.

SAITO, M. Charcoal as a micro-habitat for VA mycorrhizal fungi, and its practical implication. **Agriculture, Ecosystems and Environment**, v. 29, n. 1–4, p. 341–344, 1990.

SAITO, M.; OBA, H.; KOJIMA, T. Effect of nitrogen on the sporulation of arbuscular mycorrhizal fungi colonizing several gramineous plant species, **Soil Science and Plant Nutrition**, v. 57, n. 1, p. 29-34, 2011.

SAITO K, HASEGAWA E, SASAKI J. **The rapid diagnosis of nutritional states of crops I**. Bull. Miyagi Prefec. Agr. Exp. Cent., 55, 1–11, 1987.

SCHIMMELPFENNIG, S.; GLASER, B. One Step Forward toward Characterization: Some Important Material Properties to Distinguish Biochars. **Journal of Environment Quality**, v.

41, n. 4, p. 1001, 2012.

SINGH, B.; SINGH, B. P.; COWIE, A. L. Characterisation and evaluation of biochars for their application as a soil amendment. **Australian Journal of Soil Research**, v. 48, n. 6–7, p. 516–525, 2010.

SIQUEIRA, J. O.; HUBBELL, D. H.; MAHMUD, A. W. Effect of liming on spore germination, germ tube growth and root colonization by vesicular-arbuscular mycorrhizal fungi. **Plant and Soil,** v. 76, p. 115–124, 1984.

SMITH, S.E.; READ, D.J. **Mycorrhizal symbiosis**. 2 ed. Academic Press: London. 1997, 605p.

SOHI, S. P.; KRULL, E.; LOPEZ-CAPEL, E.; BOL, R. **A review of biochar and its use and function in soil**. 1. ed. [s.l.] Elsevier Inc., 2010. v. 105

SPARKS, D.L. **Environmental soil chemistry**. New York: Academic Press, 267 p, 1995.

SPOKAS, K. A.; NOVAK, J. M.; STEWART, C. E.; CANTRELL, K. B.; UCHIMIYA, M.; DUSAIRE, M. G.; RO, K. S. Qualitative analysis of volatile organic compounds on biochar. **Chemosphere**, v. 85, n. 5, p. 869–882, 2011.

SUN, H.; HOCKADAY, W. C.; MASIELLO, C. A.; ZYGOURAKIS, K. Multiple controls on the chemical and physical structure of biochars. **Industrial and Engineering Chemistry Research**, v. 51, n. 9, p. 3587–3597, 2012.

TAJIMA, R.; KATO, Y. A quick method to estimate root length in each diameter class using freeware ImageJ. **Plant Production Science**, v. 16, n. 1, p. 9-11, 2013.

TRIPODI, R. A. AND CHEREMISINOFF, P. N. Coal Ash Disposal Solid Waste Impacts, Technomic Publishing, Westport, CT. 1980, 52 p.

TRUOG, E. The determination of the readily available phosphorus of soils. **Agronomy Journal**, v. 22, n. 10, p. 874-882, 1930.

VITOUSEK P.M. ET AL. Nutrient imbalances in agricultural development. **Science**, v. 324, p. 1519–1520, 2009.

WARNOCK, D. D. Arbuscular mycorrhizal responses to biochars in soils - potential mechanisms of interaction and observed responses in controlled environments. Doctoral thesis, 2009, 87p.

WARNOCK, D. D.; LEHMANN, J.; KUYPER, T. W.; RILLIG, M. C. Mycorrhizal responses to biochar in soil - Concepts and mechanisms. **Plant and Soil**, v. 300, n. 1–2, p. 9–20, 2007.

ZHAO, L.; CAO, X. Heterogeneity of biochar properties as a function of feedstock sources and production temperatures. **Journal of hazardous materials**. v. 257, p. 1–9, 2013.

Supporting information

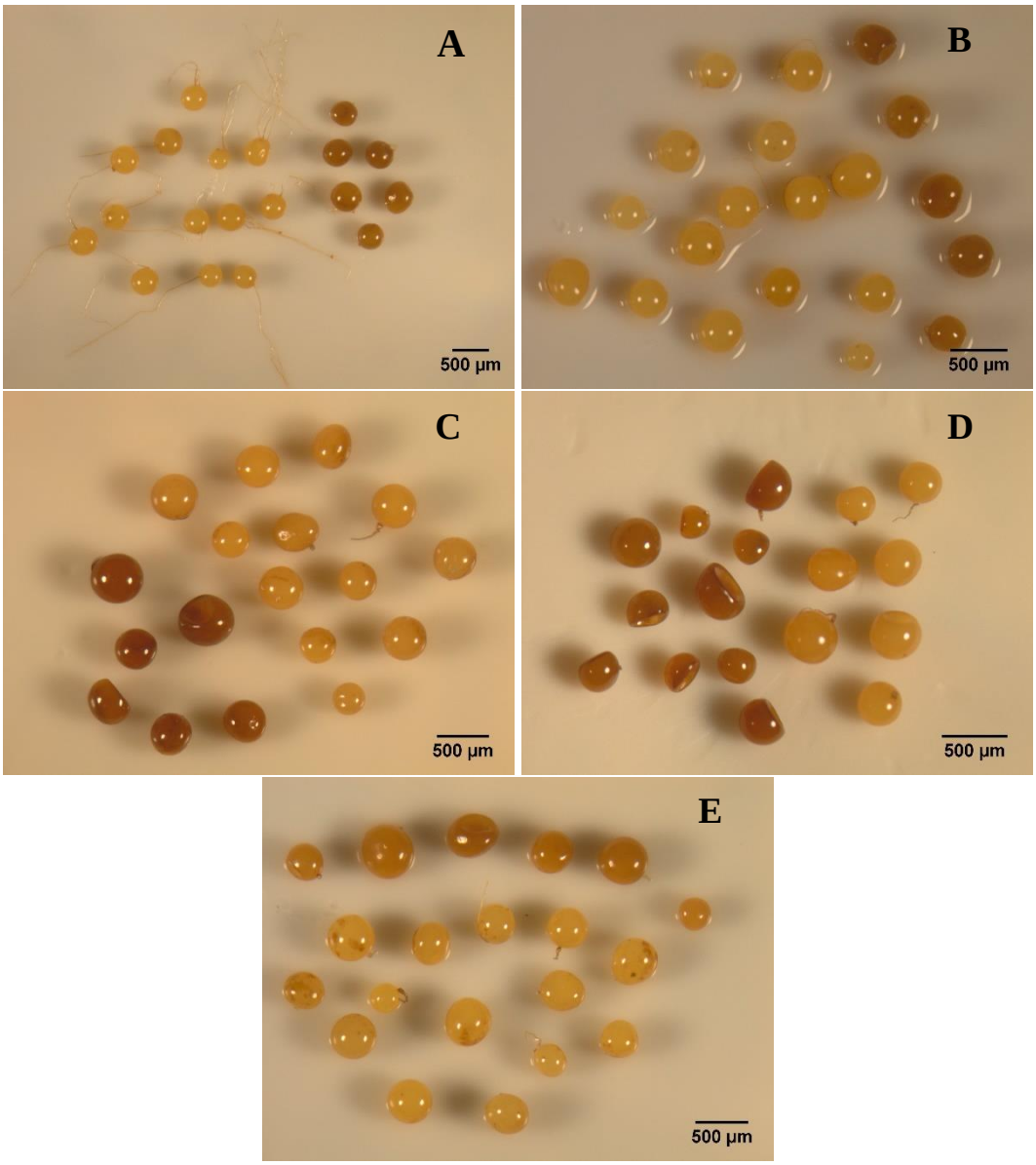

Figure S3.1 – Spore condition after two weeks of incubation in sand and soil media without (control) or with addition of biochar 300 °C or 700 °C. A: sand, control (no biochar; B: soil, control; C: sand, biochar 300 °C; D: soil, biochar 300 °C; E: sand, biochar 700 °C.

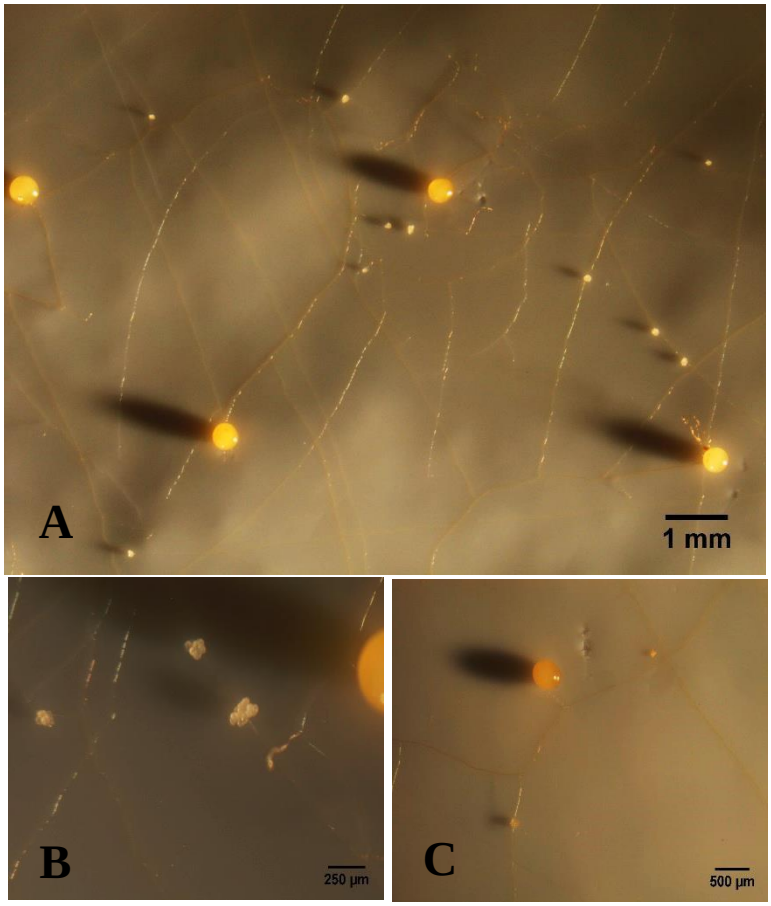

Figure S3.2 – Spores condition after two weeks of incubation in soil media with addition of biochar produced at 700 °C. A: spores, auxiliary cells and hyphae in golden color; B: detail of auxiliary cells; C: detail of spore and hyphae.

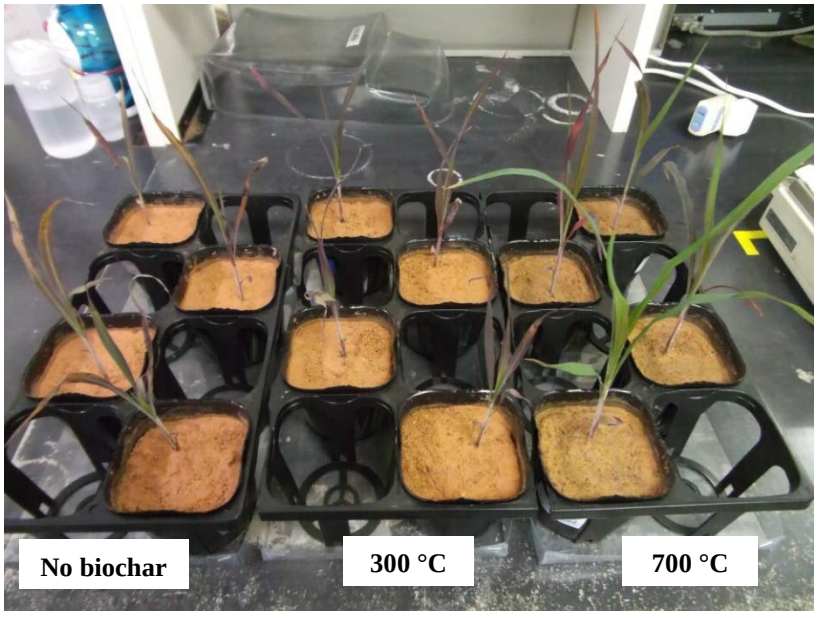

Figure S3.3 – Dwarf sorghum plants submitted to inoculation with arbuscular mycorrhizal fungi and addition of biochar, 40 days after emergence. Note that plants from 700 °C biochar treatment are greener and bigger.

FINAL CONSIDERATIONS

Our findings suggest that pyrolysis, which has gained more attention in the last 10 years, could assist us to reach a more sustainable way to produce food and treat by-products derived from agricultural activities. We utilized two different approaches: by means of pyrolysis, we produced bone-based P fertilizers, which acted as an efficient P source; and biochars, that allied to arbuscular mycorrhizal fungi assisted plants to increase their grow and nutrient (mainly P) uptake.

Pyrolysis when performed in specific conditions could generate materials (bone char and biochars) with increased effectiveness. We proved that low pyrolysis temperature is required to produce bone-based fertilizers, while high temperature of pyrolysis was more suitable for biochar production. It is important to note that pyrolysis products might vary widely according to the feedstock type employed. For example, if bones of animals of the same specie, but different ages, were used for bone char production, divergent results would be expected, reinforcing that the pyrolysis settings must be adapted to every condition (e.g. feedstock type, purpose of the use of charred material) in order to obtain the maximum benefits of the resultant material.

In the case of bone char production, we utilized synchrotron-based X-ray diffraction and XANES techniques, which helped us to discover bone char chemical characteristics. However, we suggest that a thermogravimetric analysis would be very important, at least applied to the starting material (raw bone), to better reveal the pattern of loss of compounds with increasing temperature.

Regarding the use of biochar to increase plant-AMF symbiosis, it is important to have in mind that responses to environmental changes might vary greatly depending on the AMF specie utilized. Thus, different responses related to AMF-plant symbiosis could be expected when contrasting biochars are applied to soil. For this reason, we recommend the utilization of different AMF species, biochar feedstocks, pyrolysis temperatures and soils to obtain more consistent results in studies of the same nature. The use of natural soils where AMF inoculum sources are present would best represent the current reality where most farmers do not have access to inoculants.